Endometriosis

4

Simona Mautone, Salvatore Belluardo,
Valerio Di Paola, Luigi Romano, Giovanni Foti,
Riccardo Manfredi, and Roberto Pozzi Mucelli

4.1 Endometriosis

Endometriosis is defined as the presence of endometrial tissue, composed of both glandular and stromal elements, outside of the uterine cavity.

Originally, endometriosis was further classified as endometriosis "interna" (referred to as endometrial tissue within the uterine musculature) and "externa" (endometrial tissue in all other sites). Currently, adenomyosis has replaced the term endometriosis "interna."

Several systems have been used to stage the extension of the disease. The most common staging system used is the American Fertility Society (AFS) classification. It divides the disease into minimal, mild, moderate or severe, based on the presence of ovarian or peritoneal endometriosis (subdivided into superficial or deep), adhesions, and posterior cul-de-sac obliteration [1]. The AFS classification is the most commonly used, but it has

poor correlation with severity of the disease and poor prognostic value of response to treatment. We consider the anatomic subdivision of pelvic endometriosis into three forms: the adenomyosis, the tubo-ovarian lesions (localized in the ovaries and tubes), and the deep pelvic endometriosis, defined by the invasion of endometrial tissue at least 5 mm beneath the peritoneal surface. There are also superficial peritoneal lesions, or noninvasive implants, well recognized at laparoscopy [2, 3], but usually not detectable with imaging.

4.1.1 Epidemiology

The real prevalence of endometriosis is difficult to determine since laparoscopy or surgery is required to make a definitive diagnosis [4]. Endometriosis is found especially in women of childbearing age, involved with an incidence of 10 % [5] and a peak of incidence between 24 and 29 years. Anyway it is not uncommon between adolescents (in most cases related to obstructive Mullerian duct anomalies of the cervix or vagina) [6], and about 5 % of cases are seen in postmenopausal women, related to hormone replacement therapy [7].

4.1.2 Pathogenesis

The pathogenesis of endometriosis is complex and still debated, probably multifactorial. Up to

S. Mautone (✉) • S. Belluardo • V. Di Paola
R. Manfredi • R. Pozzi Mucelli
Dipartimento di Radiologia di Verona,
Azienda Ospedaliera Universitaria di Verona,
Policlinico "G. B. Rossi", P.le L.A. Scuro 10,
Verona 37100, Italy
e-mail: simonamautone@gmail.com;
totibelluardo@alice.it; dipaola.valerio@libero.it;
rmanfredi@univr.it; roberto.pozzimucelli@univr.it

L. Romano • G. Foti
Dipartimento di Radiologia,
Ospedale "Sacro Cuore – Don Calabria",
V. don Sempreboni 5, Verona, Negrar, Italy

now, three principal theories have been proposed.

4.1.2.1 Metastatic Theory [8]

It is the most widely accepted theory that endometriosis results from a retrograde menstruation transporting endometrial tissue from the uterine cavity into the peritoneal cavity, where endometrial cells implant.

Actually, a retrograde menstruation has been observed in up to 90 % of normal women during the menstrual period [9], but endometrial tissue is normally resorbed by the abdominal cavity. Instead in case of endometriosis, the equilibrium between retrograde menstruation and resorption of endometrial tissue in the abdominal cavity is altered and leads to development of endometriosic lesions. Further evidence of this theory is suggested by the major frequency in women with obstructive anomalies of Mullerian duct development and with consequently excessive retrograde flow [6] and by the anatomic locations of the disease in the dependent pelvic areas [10]. Furthermore, the risk of endometriosis seems to be dependent on the amount of menstrual flow.

The metastatic spread can happen also by vascular and lymphatic channels or iatrogenically during surgery.

4.1.2.2 Metaplastic Theory [11]

It suggests the metaplastic differentiation of the Müllerian remnant tissue or peritoneal cells of serosal surfaces into functioning endometrial cells. The demonstration of endometriosis in women lacking functional eutopic endometrium (e.g., Turner syndrome, uterine agenesis) supports this theory [12].

4.1.2.3 Induction Theory

This is a combination of both first two theories. It suggests that substances released from shed endometrium induce undifferentiated mesenchyma to form endometriosic tissue [6].

Regardless of these theories, there is growing evidence suggesting that a genetic component plays a role in endometriosis with significant familial clustering and first-degree relatives of women with endometriosis having a sevenfold greater chance of having endometriosis [13].

Table 4.1 Symptoms related to anatomic location of endometriosic implants

Anatomic location	Symptoms
Pouch of douglas, torus uterinus, USLs, rectovaginal septum	Dyspareunia
Bowel	Dyschezia, catamenial diarrhea, rectal bleeding, constipation, intestinal occlusion
Ureteral stenosis	Urinary obstruction, flank pain
Bladder	Urgency, frequent urination, hematuria
Pleura – lung	Hemophthysis, chest pain, shortness of breath
Brain	Perimenstrual headaches, seizures, subarachnoid hemorrhage
Skin	Catamenial bleeding, tenderness

4.1.3 Signs and Symptoms

Endometriosis is frequently asymptomatic; it could be associated with a wide variety of symptoms, none of these pathognomonic, thus making the diagnosis difficult.

The most important clinical manifestations are pelvic pain and infertility. Endometriosis was detected at surgery in 19 % of women with chronic pelvic pain. Patients usually have cyclic symptoms related to bleeding and inflammation of menses; common symptoms are dysmenorrhea, back pain, dyspareunia, and rectal discomfort. However, clinical manifestations are related to implant's location and are listed in the Table 4.1.

Infertility may be the presenting complaint of endometriosis, with or without pelvic pain. It is estimated that 30–50 % of women with endometriosis are infertile, and 20 % of infertile women have endometriosis [14]. The pathogenic mechanism is debated. It could be related to repeated episodes of bleedings causing a chronic inflammatory state, which can lead not only to anatomic alterations induced by fibrosis and adhesions, but also to bio-humoral changes [15].

Of the three forms, deep pelvic endometriosis is thought to contribute most often to clinical symptoms. Then, in case of ovarian endometrioma

with chronic and severe pelvic pain, associated deep pelvic endometriosis lesions are generally present, often multifocal and with intestinal infiltration [16].

4.1.4 Diagnosis

The lack of specific symptoms makes the diagnosis of endometriosis difficult and, often, very late. Diagnosis is made harder because the first-line imaging study, usually transvaginal or transabdominal ultrasound (US) [17], has a high sensitivity for adnexal lesions but a poor accuracy for other locations, especially for deep pelvic endometriosis, frequently giving false-negative results [17]. Above transabdominal and transvaginal US, several techniques have been used: magnetic resonance (MR) imaging and, in case of suspected bowel endometriosis, transrectal ultrasonography (US), rectal endoscopic sonography, and double barium contrast enema (DBCE). When the urinary system is involved, MR urography and cystography could be employed.

The reference standard for the diagnosis of pelvic endometriosis remains laparoscopy with histological confirmation.

In this chapter, we would highlight the role of magnetic resonance (MR) imaging in the diagnosis of endometriosis. This technique has already been demonstrated as a successful diagnostic tool to investigate the tubo-ovarian endometriosis, with a sensitivity, specificity, and accuracy of 90, 98, and 96 %, respectively [18], but also for deep endometriosis, with a sensitivity and specificity of 90 and 91 %, respectively [19].

4.2 Uterine Adenomyosis

Adenomyosis is a common non-neoplastic uterine disease defined by the presence of ectopic endometrial tissue within the myometrium, due to the invagination of endometrium in the myometrium at a depth of at least 2.5 mm below the basal layer of the endometrium. This process leads to hyperplasia and hypertrophy of the smooth muscle [20].

Adenomyosis can be either *focal* (one or several foci in the myometrium) or *diffuse* (numerous foci spread throughout the myometrium), and it is often asymmetric, predominating in the posterior uterine corpus. More controversial is the distinction between *superficial* (simple thickening of the junctional zone seen on MRI or lesions not extending beyond one third of the depth of the myometrium) and *deep forms* (penetrating deeper than one third of the myometrium). Although it has been accepted that uterine adenomyosis results from the direct invasion of the endometrium into the myometrium, and in such cases no direct relationship between the adenomyosis and the endometrium is proved histologically. Rather the disease appears to be the result of the invasion of endometrium-like structures (presumably endometriosis) from outside the uterus, disrupting the uterine serosa. This case has been named by some authors as "*external*" (or "extrinsic") adenomyosis, connected to lesions of deep pelvic endometriosis [21] extending to the uterine myometrium, frequently sparing the endometrial-myometrial junctional zone. The definition of this form as "external" adenomyosis or DPE involving the uterus is still debated; however, it practically does not affect therapy.

Furthermore, in some cases adenomyosis is present in the myometrium completely isolated from both the endometrium and the serosa. Such a difference would postulate a new hypothesis that adenomyosis is composed of multiple heterogeneous subtypes [22].

4.2.1 Imaging Features of Adenomyosis

4.2.1.1 Ultrasonography

The transvaginal ultrasonography (TVUS) is usually the first-line investigation in cases of suspected adenomyosis. The transabdominal ultrasonography has a poor sensitivity (53–89 %) but a good specificity (97 %). The combination of transabdominal and transvaginal ultrasonography (TVUS) increases the diagnostic accuracy.

The direct signs of adenomyosis are:

1. Anechoic subendometrial microcysts in the myometrium (2–4 mm) that can be distinguished from vascular images on

Doppler sonography because they are not vascularized (pathognomonic sign). This cystic space corresponds to ectopic dilated endometrial glands into the myometrium; if they are hemorrhagic, their content shows greater echogenicity.

2. Inhomogeneous appearance of the myometrium with hyperechoic linear striations (correlated to its hypertrophy).
3. Small hyperechoic subendometrial nodules, pseudonodular hypoechoic zones with indistinct contours and no mass effect on the endometrium.
4. A poorly defined or thickened endometrial-myometrial junctional zone (JZ).

   The indirect signs of adenomyosis are:

1. The uterus is enlarged, rounded with regular contours.
2. Asymmetric thickening of the myometrium, especially in case of focal adenomyosis, results from reactive hyperplasia and hypertrophy of the smooth muscle fibers around the ectopic endometrial glands.
3. Linear pattern of vascularization on Doppler sonography, crossing the myometrium within the adenomyosic lesion (opposed to the leiomyoma).
4. A poorly defined or thickened endometrial-myometrial junctional zone (JZ).

4.2.1.2 Magnetic Resonance Imaging (MRI)

Pelvic MRI is the second-line investigation, and it offers the best performance when there is any doubt over diagnosis and in terms of looking for any pathology associated with adenomyosis.

Pelvic MRI is superior to TVUS in terms of sensibility and specificity for both focal and diffuse adenomyosis.

The MRI signs of adenomyosis can be classified into direct and indirect.

The *direct MRI signs* of adenomyosis are:

1. On T2-weighted images, typical adenomyosis appears as an ill-demarcated low-signal-intensity area (Fig. 4.1a, c, e, f), owing to abundant smooth muscle proliferation, with or without punctuate high-signal-intensity foci scattered throughout the lesion or high-signal-intensity linear striations extending from the endometrium. Hyperintense foci could be present on T1-weighted images, more evident with fat saturation, corresponding to small areas of hemorrhage (Fig. 4.1b, d).
2. An important sign of adenomyosis is the presence of subendometrial microcysts, related to the presence of endometrial glands within the myometrium. MRI reveals round cystic foci varying from 2 to 7 mm in diameter, hyperintense on T2-weighted sequence, embedded within the myometrium, and usually located within the JZ. Sometimes, at the end of the menstrual period, hemorrhagic foci within cystic cavities are recognizable and appear as high-signal-intensity spot on T1-weighted images owing to the T1-shortening effects of methemoglobin. This hemorrhagic content is not found routinely because adenomyotic endometrium, like the basalis endometrium, seldom responds to hormonal stimuli with cyclic changes, but it is less common than in endometriosis. Susceptibility-weighted imaging (gradient echo – GRE sequences) is sensitive for old hemorrhagic foci, which appear as spotty signal voids owing to the T2*-shortening effects of accumulated hemosiderin.

At diffusion-weighted images, adenomyosis has low to intermediate signal intensity, a finding consistent with its benign, non-neoplastic nature. Because adenomyosis may show various degrees of enhancement after administration of contrast medium, dynamic study does not contribute to diagnostic accuracy. However, additional MR angiographic GRE sequences are recommended in patients with adenomyosis in whom uterine artery embolization is planned.
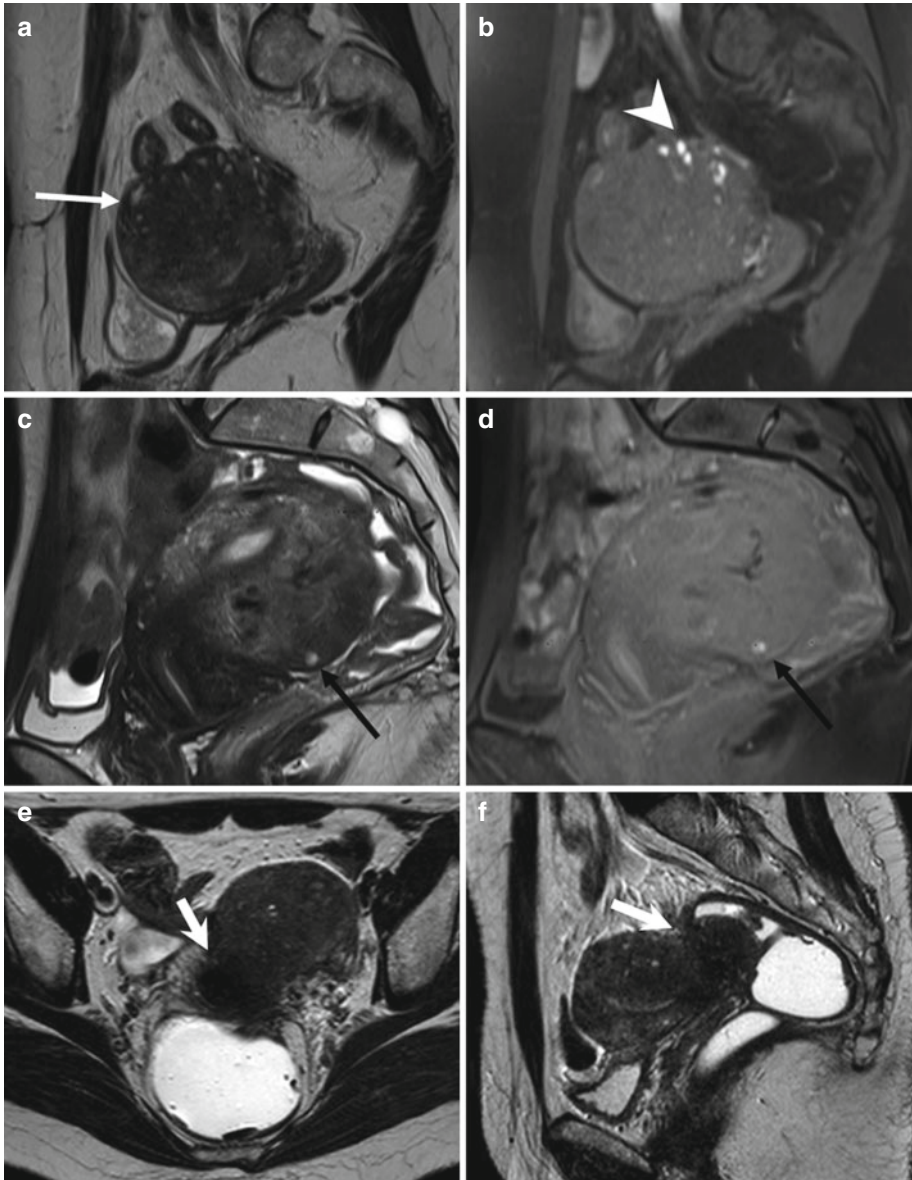
Fig. 4.1 Diffuse adenomyosis. Sagittal (**a**, **c**, **f**) and axial (**e**) T2-weighted FSE images. Sagittal T1-weighted FS-GRE image (**b**, **d**). **a** (TR 4670 TE 94), **b** (TR 369, TE 10). The uterus is markedly enlarged, especially in the posterior portion, with regular contours and a thickened and poorly recognizable endometrial-myometrial junctional zone (JZ). On T2-weighted images this low-signal-intensity area contains multiple small foci hyperintense (**a**: *arrow*), which represent ectopic endometrial glands and small subendometrial cysts. The high-signal-intensity spots on T1-weighted fat-saturated image (**b**: *arrowhead*) correspond to multiple area of hemorrhage within the ectopic endometrial tissue. **c** (TR 3870 TE 100), **d** (TR 369, TE 10). The uterus is retroflexed and markedly enlarged in its posterior portion, with hyperintense spots in both T1- and T2-weighted images (*black arrow*). These findings are consistent with adenomyosis. **e** (TR 4530 TE 90), **f** (TR 5390 TE 113). Also in this case the uterus is enlarged, and the JZ is thickened. Moreover a heterogeneous hypointense nodule on T2-weighted images is recognizable in the pouch of Douglas (*short arrows*), suggestive of deep pelvic endometriosis (DPE) location. Obliteration of the fat tissue plan and invasion of both the posterior uterine surface and anterior rectosigmoid wall are present
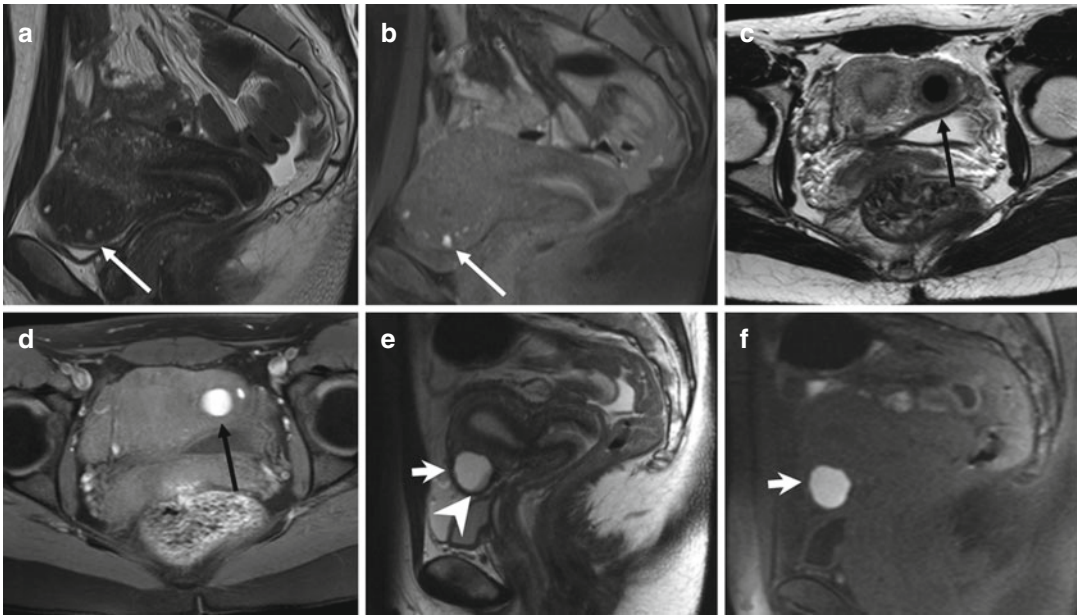
Fig. 4.2 Focal adenomyosis (**a**, **b**). Sagittal T2-weighted (**a**: TR 4070, TE 94) and FS-T1-weighted (**b**: TR 629, TE 10) images. The uterus is anteverted. A focal myometrial thickening is recognizable on the anterior uterine wall (*arrows*). This area is heterogeneously hypointense on T2-weighted image, with hyperintense foci on both T1- and T2-weighted sequences, findings consistent with focal uterine adenomyosis. Adenomyotic cysts. Two cases. (**c**, **d**) Axial T2-weighted FSE MR image (**c**: TR 3252, TE 100) and axial T1-weighted fat-suppressed image (**d**: TR 629, TE 10) show a rounded well-defined intramyometrial lesion (*black arrow*), located near the left uterine horn. This lesion shows a very low signal intensity on T2-weighted sequence (**c**) and high signal intensity on T1-weighted image (**d**), related to its hemorrhagic content. (**e**, **f**) Sagittal T2-weighted FSE MR image (**e**: TR 4530, TE 90) shows another adenomyotic cyst, located in the subserosal layer of the anterior uterine wall, with inhomogeneous high signal intensity content (*short arrow*) and contextual-dependent fluid-fluid level (*arrowhead*). This cyst retains high signal intensity on T1-weighted fat-suppressed MR image (**f**: TR 328, TE 11), due to its hemorrhagic content

The indirect signs of adenomyosis are secondary to the reactive hyperplasia of the myometrium provoked by endometrial invasion and include:

1. Globular aspect of the enlarged uterus with regular contours.
2. Asymmetric thickening of the myometrial walls (more common of the posterior wall).
3. Thickening of endometrial-myometrial junctional zone (JZ: Fig. 4.1). Generally, a JZ thickness of greater than 12 mm is the accepted criterion in establishing the presence of adenomyosis (JZ ≥12 mm). Also the greatest JZ thickness to total myometrium ratio >40–50 % is considered [23]. However, adenomyosis can be excluded if the JZ thickness is 8 mm or less [24]. Anyway, from 20 to 30 % of patients will not have a visible or measurable endometrial-myometrial junctional zone during their reproductive cycle [25].

4.2.2 Atypical Morphologic Appearances of Adenomyosis

4.2.2.1 Adenomyoma

Adenomyoma is an atypical morphologic appearance of adenomyosis and is rarer than both focal and diffuse adenomyosis. It is composed of a focal consolidation of adenomyotic glands and appears as a poorly defined nodular lesion with extensive muscular response (Fig. 4.2a, b). It may be intramyometrial, subserosal, and possibly even intracavitary. Like adenomyosis, adenomyoma

usually shows heterogeneous low signal intensity on T2-weighted images and may be indistinguishable from degenerated leiomyomas and from aggressive uterine neoplasms such as uterine sarcomas. Relatively low signal intensity at diffusion-weighted imaging with high ADC value is suggestive of its benign nature.

4.2.2.2 Adenomyotic Cyst

Adenomyotic cyst (cystic adenomyosis) is a rare variation of adenomyosis that appears as an intramyometrial endometrioma-like lesion, hyperintense on T1-weighted images, surrounded by adenomyotic tissue with low signal intensity on T2-weighted images (Fig. 4.2c–f). A subserosal adenomyotic cyst may mimic an ovarian tumor. The finding of continuity with the myometrium is suggestive of its uterine origin [26].

4.2.3 Malignant Transformation of Adenomyotic Lesions

Malignant transformation of adenomyosis is quite rare and may manifest as a predominantly intramyometrial mass. Imaging findings of an adenomyotic cyst with malignant transformation are similar to those of an endometrioma with malignant transformation. High-signal-intensity hemorrhagic fluid in the adenomyotic cyst on T1-weighted images may mask the enhancement of malignant mural nodules; therefore, contrast-enhanced subtraction imaging may be useful for detection of malignant transformation. Dynamic contrast-enhanced imaging may have greater accuracy than T2-weighted imaging when adenomyosis and endometrial cancer coexist [27]. Diffusion-weighted imaging can demonstrate the malignant foci as areas of high signal intensity.

4.2.4 Differential Diagnosis

Various benign and malignant conditions may mimic adenomyosis: physiologic myometrial contraction, myometrial involvement by deep pelvic endometriosis, leiomyomas, low-grade endometrial stromal sarcoma, and myometrial metastases.

Transient myometrial contraction is a physiologic phenomenon that may mimic focal adenomyosis because it determines focal pseudo-thickening of the junctional zone. This aspect usually disappears on subsequent images or at cine MR images, instead of focal adenomyosis that persists.

Myometrial contractions in the pregnant uterus are commonly seen and usually do not represent a diagnostic dilemma.

To differentiate physiologic myometrial contractions from focal adenomyosis, rapid T2-weighted sequences can be repeated and should be correlated with other views. Useful to eliminate physiologic uterine contractions is the injection of an antiperistaltic drug, if no contraindications are present.

4.3 Ovarian Endometriosis

The most common location of endometriosis is the ovary, where small and shallow endometrial implants develop, leading to adjacent para-ovarian scarring and adhesions. An ovarian enlargement could be present, attributable to repeated episodes of hemorrhage within a deep implant, resulting in endometriosic cysts, also defined as *endometriomas* (multiloculated cystic lesions). They may completely replace normal ovarian tissue. From the anatomo-pathological point of view, endometriosic cyst walls are generally thick and fibrotic with common areas of discoloration and dense fibrous adhesions. The cyst lining can vary from smooth and pale to shaggy and brown. Their contents can be watery or, more typically, composed of thick, dark, degenerated blood products, depending on the presence and dating of bleeding. This appearance is called "chocolate cyst."

4.3.1 Ultrasonography

Pelvic ultrasound (especially TVUS) is the method of choice to identify endometriomas, defined as benign ovarian neoplasms persisting
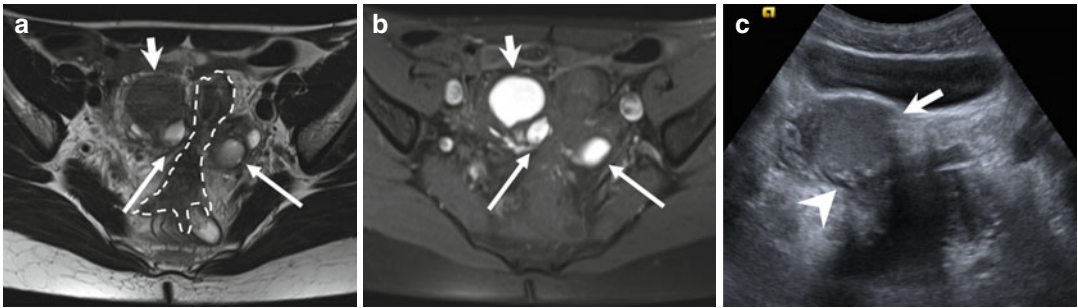
Fig. 4.3 "Kissing ovaries" and bowel adhesions due to endometriosis. Axial T2-weighted FSE MR image (**a**: TR 4070, TE 94) shows small bilateral ovarian cysts of intermediate signal intensity (*arrows*) and one right-sided ovarian cyst (*short arrow*) with marked "T2-shading effect" (low signal intensity). Correspondent axial T1-weighted fat-suppressed MR image (**b**: TR 351, TE 10) shows bilateral T1-hyperintense endometriomas (*arrows* and *short arrow*), confirming the hemorrhagic nature of the cystic content. Adhesions between bilateral endometriomas bring the ovaries closer to the midline ("kissing ovaries" sign). Furthermore there is tight contact with obliteration of the fat tissue plane between ovarian masses and the interposed sigmoid colon (**a**: *dashed line*), due to adhesions related to endometriosis. Transverse transabdominal sonogram (**c**) demonstrates the right-sided endometrioma (*short arrow*) with diffuse low-level internal echoes and focal wall hyperechoic nodularities (*arrowhead*)

after 3 months. They typically appear as multilocular cysts with diffuse low-level internal echoes and hyperechoic foci in their walls (Fig. 4.3c). Internal thin or thick septations may be present. However, unilocular cysts were found in 43 % of endometriomas. The echogenic wall foci differ from true wall nodules because they are more echogenic and smaller than malignant wall nodules. Although the pathological basis of their formation has not been established, it is postulated that they form as cholesterol deposits accumulating in the endometrioma's wall.

The endometriomas vary between 30 and 59 mm in maximum diameter in 81 % of cases. The positive predictive value of sonography to predict ovarian endometriosis was evaluated at 75 % when criteria such as diffuse low-level internal echoes and absent neoplastic features were used [28]. The color Doppler imaging shows the absent flow within the lesion. The presence of hyperechoic foci alone at the surface of the ovary is not a sign for endometriosis.

Differential diagnosis includes ovarian functional cysts, mature cystic teratoma, cystadenoma, fibroma, tubo-ovarian abscess, and ovarian carcinoma. The functional cysts, such as corpus luteum or hemorrhagic follicular cysts, will disappear or decrease in size at short-time follow-up. Ovarian cancer can be difficult to exclude if

wall irregularities or nodules are present; absence of color Doppler flux within the cyst helps to confirm the benign nature of the lesion. Whenever sonographic features of ovarian masses are uncertain or indeterminate, MRI is the imaging modality of choice to rule out malignancy.

4.3.2 MRI Findings

Superficial peritoneal ovarian endometriosis, not visible at TVUS, can be only rarely detected by MRI, using fat-suppression techniques, as hemorrhagic superficial foci [2]. Their signal intensity is quite variable [3].

Instead *endometriomas* have typical MRI features, and this technique has a sensitivity and specificity reported of 90 and 98 %, respectively, in the definitive diagnosis [29]. Endometrioma appears as a cystic mass with internal high signal intensity on T1-weighted images, also with fat suppression (Figs. 4.3, 4.4, and 4.5). The walls are usually thickened, and, frequently, loss of the interface between lesion and adjacent organs is present (Fig. 4.3).

Use of chemically selective T1-weighted fat-suppressed sequences is mandatory to visualize smaller endometriomas and to differentiate endometriomas from mature cystic teratomas
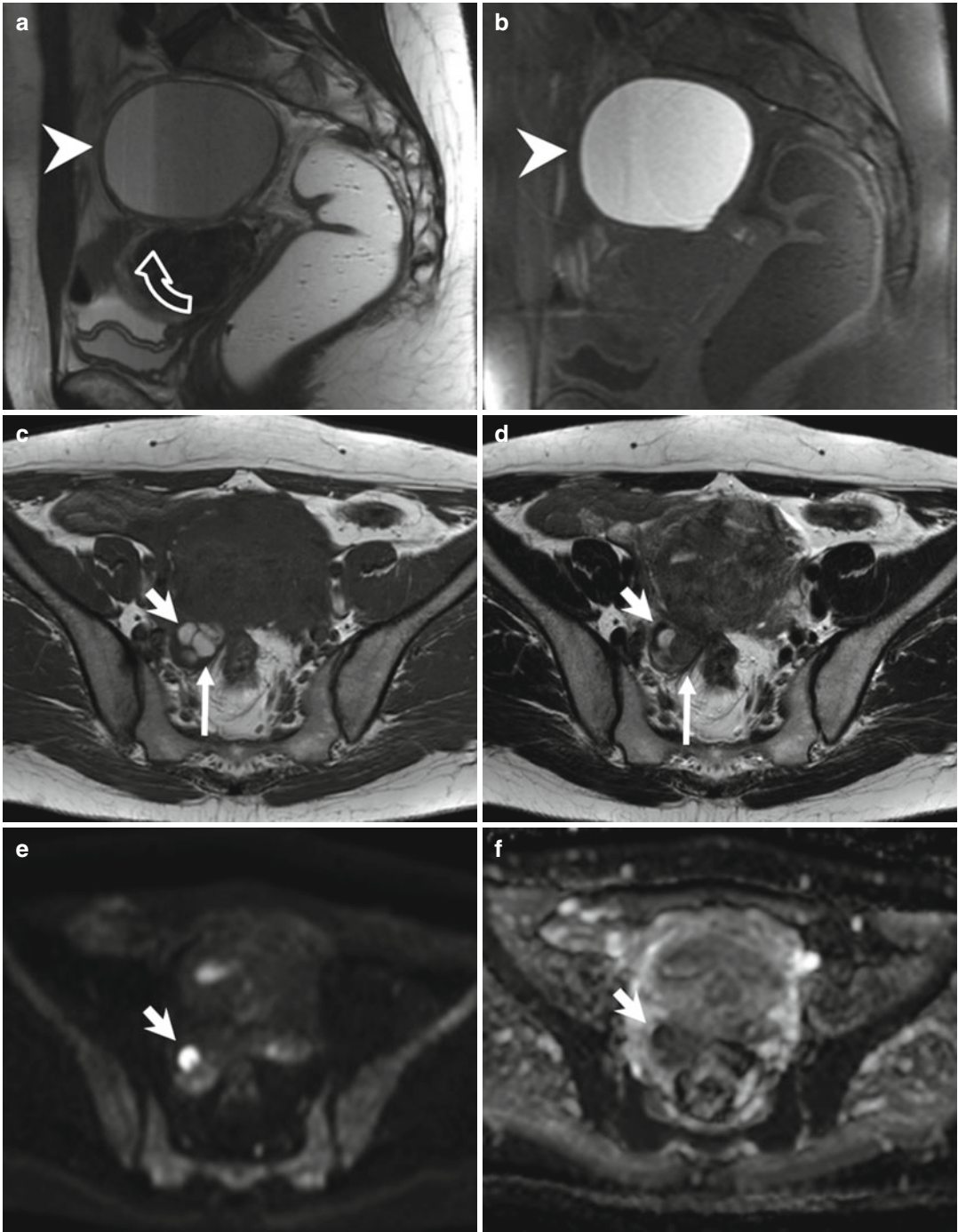
Fig. 4.4 Large endometrioma (**a**, **b**). Sagittal T2- (**a**: TR 4530, TE 90) and T1-FS-weighted (**b**: TR 328, TE 11) images show a large adnexal cystic lesion (*arrowheads*) with fluid-fluid level (**a**: *curved arrow*). The dependent component appears hyperintense on T1-weighted image with fat suppression (**b**) and shows a marked T2-shading effect (hypointensity on T2-weighted image). Small endometriomas (**c–f**). Axial T1-weighted FSE MR image (**c**: TR 640, TE 10) shows multiple small T1-hyperintense cystic lesions in the right ovary. Axial T2-weighted FSE MR image (**d**: TR 3652, TE 100) at the same level shows marked T2 shading (hypointensity) in the posteromedial cystic lesion of the right adnexa (*long arrows*), instead of the anterolateral cyst (*short arrows*), hyperintense on both T1- and T2-weighted images. Furthermore only the anterolateral cyst (*short arrows*) presents a restricted diffusion, seen in almost half of endometriomas: in the correspondent diffusion-weighted MR image obtained with *b* value of 800 s/mm^2 (**e**: TR 7198, TE 69), it shows high signal intensity (*short arrow*) with low signal intensity on the ADC map (**f**: TR 7198, TE 69)
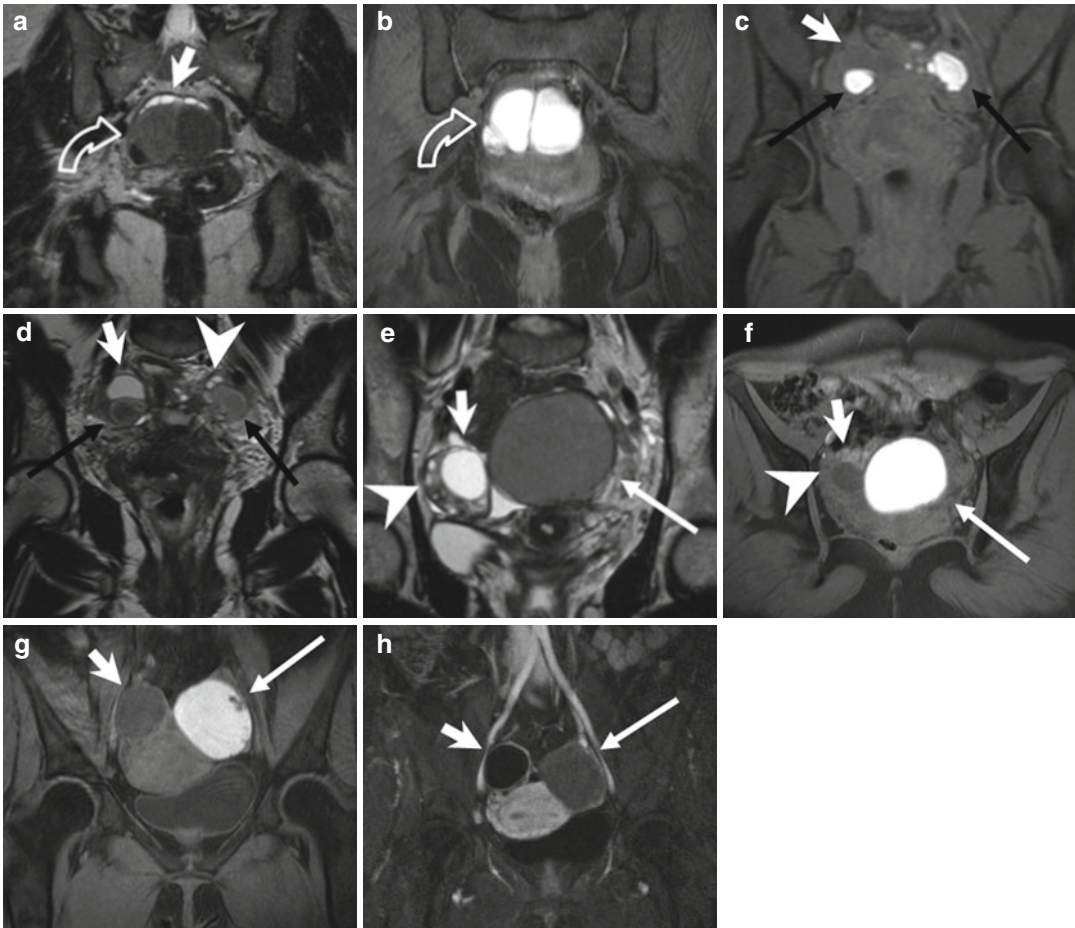
Fig. 4.5 Endometriomas (**a**, **b**) Coronal T2-weighted FSE (**a**: TR 5390, TE 113) and fat-suppressed T1-weighted (**b**: TR 440, TE 4.9) FSE MR images show multiloculated adnexal cystic mass with a "coffee bean" appearance (*curved arrow*). These cystic formations present high signal intensity on T1-weighted fat-suppressed MR image (**b**) and marked "T2-shading effect" with consequent lower signal intensity than the adjacent functional ovarian follicles on T2-weighted image (**a**: *short arrow*). Bilateral endometriomas (**c**, **d**). Coronal fat-suppressed T1-weighted FSE image (**c**: TR 597, TE 11) and T2-weighted FSE image (**d**: TR 3520, TE 89). Bilateral endometriomas (*black arrows*), hyperintense on T1-weighted sequence, present the typical "shading sign" on the T2-weighted image (**d**: *black arrows*). Furthermore a hypointense functional cyst (*short arrow*) is present in the right adnexa and multiple ovarian follicles in the left (*arrowhead*), both hypointense on T1- and hyperintense on the T2-weighted images. (**e**–**h**) Endometrioma of the left ovary. Coronal T2-weighted FSE (**e**: TR 5390, TE 113), axial T1- (**f**: TR 493, TE 4.9) and coronal T1-weighted with fat suppression (**g**: TR 440, TE 4.9) MR images show the two ovaries adjacent to the midline (the "kissing ovaries sign"). A functional cyst (*short arrow*) and multiple ovarian follicles (*arrowhead*) are recognizable in the right ovary, both hyperintense on T2- and hypointense on T1-weighted images. In the left ovary an endometrioma presents some parietal nodules (**g**: *arrow*), feature suspected for malignant degeneration. The coronal contrast-enhanced T1-weighted fat-suppressed MR image (**h**: TR 3.7, TE 1.3) demonstrates no contrast uptake within the parietal nodules (*arrow*), ruling out the suspect of malignant degeneration

(hypointense after fat saturation, due to their fat content).

Gradual decrease of signal intensity at T2-weighted image has been described as "T2-shading" sign and is due to chronic bleeding with high concentrations of iron and protein inside the endometriomas (Figs. 4.4a, d and 4.5a, d, e). Adnexal mass with high signal intensity on T1-weighted fat-saturated sequences and signal intensity lower than that of simple fluid on T2-weighted images helps to establish a diagnosis of endometrioma, with a specificity greater than 90 %.

The differential diagnosis with functional hemorrhagic cysts is not always simple. The functional cysts do not demonstrate (or demonstrate less) T2-shading sign and disappear at follow-up imaging. Bilaterality and multifocality of adnexal lesions, along the other characteristics above discussed, can help establish the diagnosis of endometrioma. Bilateral endometriomas occur in more than 50 % of cases, often associated with interovarian adhesions, described as "kissing ovaries" sign (Figs. 4.3 and 4.5e–h). When atypical features of endometriomas are present, such as localized wall thickening, the use of intravenous contrast media is mandatory: the absent enhancement confirms the benign nature of the disease.

At contrast-enhanced T1 sequences (Fig. 4.5h), the peripheral hypointense rim of the endometrioma, representing the thick fibrous capsule, usually shows intense enhancement. Instead the enhancement of solid nodules within a hemorrhagic ovarian cyst has been described in case of ovarian cancer arising within endometrioma [30].

Diffusion-weighted imaging (DWI) with quantitative assessment of apparent diffusion coefficient values (ADC) has often been incorporated into pelvic MR imaging protocols (Fig. 4.4e, f), even though the presence of restricted diffusion and low ADC value within an adnexal lesion does not have a high positive predictive value or specificity for the diagnosis of ovarian malignancy. Benign hemorrhagic ovarian cysts, endometriomas, and solid endometrial implants, as well as benign mature cystic teratomas, also can demonstrate restricted diffusion [31–33].

During pregnancy, increased progesterone levels promote hypertrophy of the endometrial stromal cells and formation of the vascular decidual lining of the uterus. Endometrial stromal cells within endometriomas may also respond to hormonal changes forming vascularized mural nodules. Decidualized endometriosis can mimic ovarian cancer at US and MR imaging. An MR imaging feature specific for decidualized endometriosis is the T2 hyperintensity of the mural nodules, isointense to the thickened decidualized endometrium, and with a broad base. After the end of the pregnancy, decidualized endometriosis has been reported to either resolve or regress to uncomplicated endometriomas (Fig. 4.6) [34].

4.3.3 Malignancies Arising in Endometriomas

Women with endometriosis are at risk for developing both clear cell and endometrioid subtypes of epithelial ovarian cancer. An estimated 2.5 % of women with endometriosis develop an ovarian cancer that usually manifests at an earlier stage, with a lower grade and a better prognosis than ovarian malignancies in women with no endometriosis [33, 35].

Endometriosis is one of several benign causes of an abnormal cancer antigen 125 (CA-125) level; thus, an elevated biomarker value alone is not specific for endometriosis-associated ovarian cancer.

The MR imaging features suggestive of malignant endometriomas are the increase in size and, more specific, the development of enhancing mural nodules.

Dynamic subtraction MR imaging is useful in depicting small contrast-enhanced nodules within the hyperintense endometrioma on T1-weighted images. Normal adjacent ovarian parenchyma, intracystic coagulate, inflammation, and decidual change of the endometrium in an endometrioma during pregnancy should be differentiated from malignant transformation. The adjacent ovarian parenchyma may be mistaken for a contrast-enhanced solid malignant component in an endometrioma. An extracystic crescent-shaped
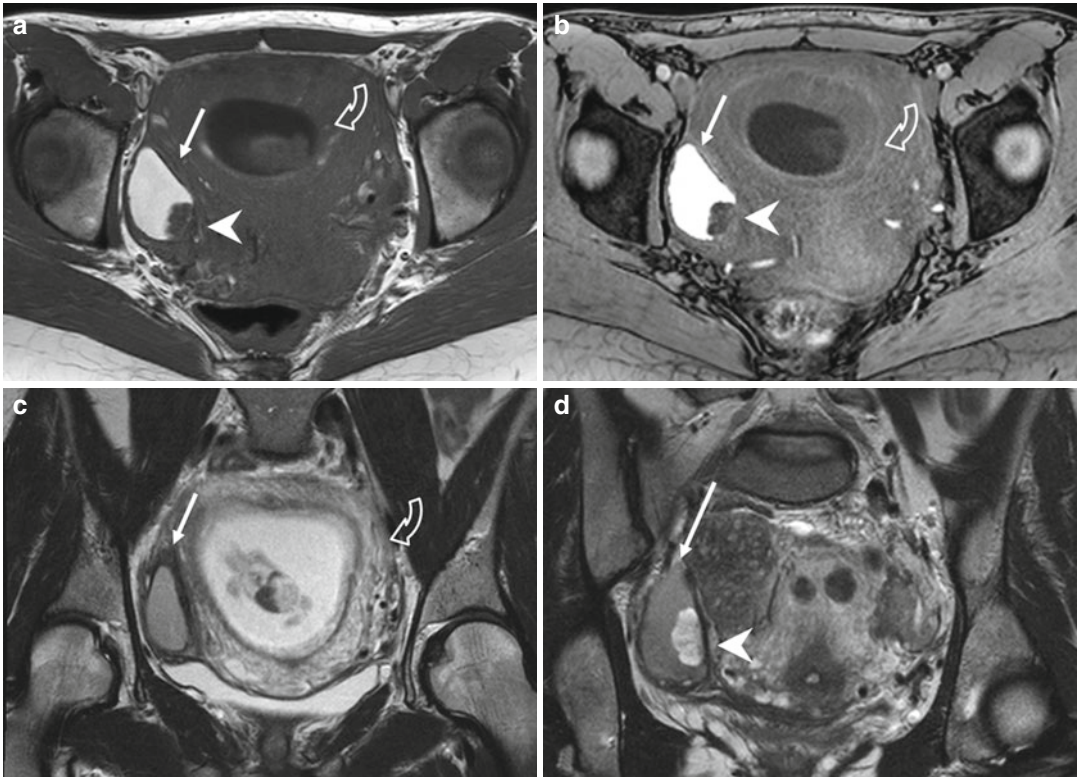
Fig. 4.6 Endometrioma with mural nodule due to decidual reaction of pregnancy (**a**–**d**). Axial T1-weighted (**a**: TR 642, TE 10), FS-T1-weighted (**b**:TR 5,8 TE 2,8), and T2-weighted images (**c**, **d**: TR 4251, TE 100) of a pregnant woman show an enlarged gravidic uterus (*curved arrows* due to decidual reaction due to pregnancy) and a hyperintense cystic lesion (*arrows*) in the right ovary. In the posterior part of this cystic formation, a mural nodule (*arrowheads*) is visible, hypointense on the T1-weighted images, and hyperintense on the T2-weighted sequence. It is a decidualized endometriosis location, related to the hypertrophy of the endometrial stromal cells in the endometrioma. It was due to the increased progesterone levels during pregnancy, and it completely regressed on the MRI images obtained 6 weeks postpartum, when only the endometrioma remained visible

portion, which may contain follicles, is the characteristic finding in such cases [33, 35].

4.3.4 Endometriosis of the Fallopian Tubes

Endometriosis is a frequent cause of dilated fallopian tubes; 30 % of women with endometriosis show tubal involvement at laparoscopy. The fallopian tubes are involved by endometrial implants in 6 % and by adhesions in 24 % of cases.

Tubal endometriosis can be divided into two forms, on the basis of implant location: the *serosal/subserosal* and the *intraluminal* forms. Both types of tubal endometriosis can be either unilateral or bilateral. The most common *serosal* or *subserosal* endometriosis is characterized by implantation of endometrial tissue on the peritoneal surface of the fallopian tubes. Recurrent hemorrhages within the serosal implants presumably result in fibrosis and scarring, leading to peritubal adhesions, obstruction of the tube, and hydrosalpinx.

The *intraluminal endometriosis* is less common and involves ectopic implantation of endometrium on the mucosal surface of the tube lumen. Cyclic hemorrhage of the implants can cause distention of the fallopian tube with blood, resulting in a hematosalpinx. Hematosalpinx has been reported to be one of the indicators of pelvic endometriosis, and it may be the only imaging finding indicative of endometriosis. However,
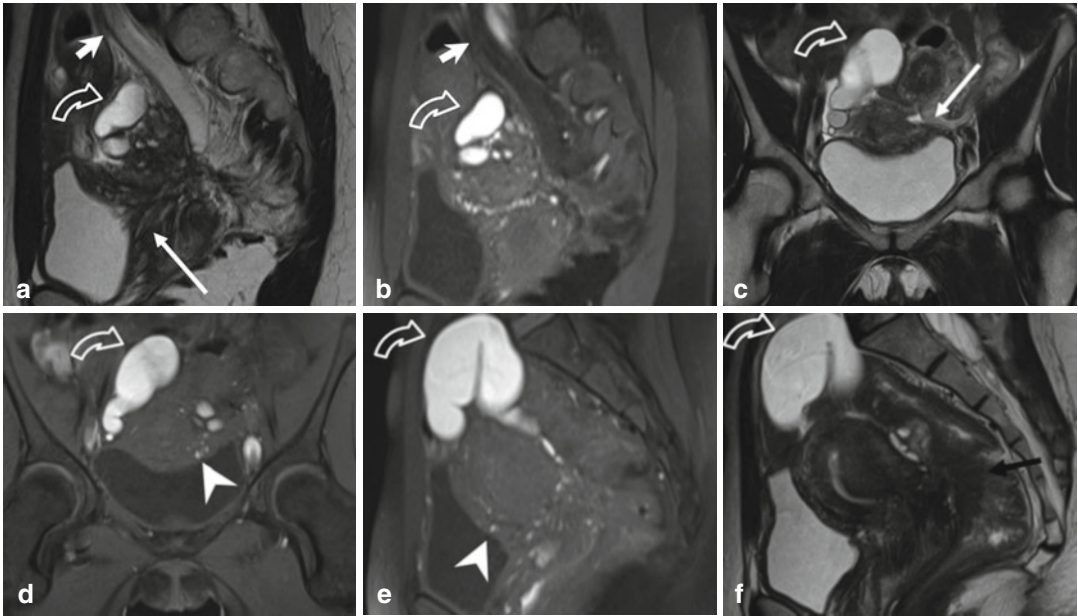
Fig. 4.7 Extensive deeply infiltrating endometriosis involving the urinary system. Sagittal (**a**, **f**) and coronal (**c**) T2-weighted MR images (TR 4670, TE 94). Sagittal (**b**, **e**) and coronal (**d**) T1-weighted fat-suppressed images (TR 369, TE 10). A deep pelvic lesion involves both the anterior and the posterior pelvic compartment; it is located over the bladder dome (**a**, **c**: *arrows*) with obliteration of the vesicouterine pouch (*extrinsic bladder endometriosis*). Also the distal portion of the left ureter is encased by the endometriosic lesion, with an upstream ureteral dilatation (**a**, **b**: *short arrows*). Intralesional small hyperintense foci on T1-weighted images (**d**, **e**: *arrowheads*) represent microhemorrhages in the ectopic endometrial glands. Bilateral hematosalpinx (*tubal endometriosis: curved arrows*), more evident on the right fallopian tube, coexists. Also obliteration of the pouch of Douglas and infiltration of the anterior rectal wall (**f**: *black arrow*) are present

hematosalpinx is not specific for endometriosis and may have other causes, such as tubal pregnancy, tumors, and tubal torsion. So an accurate assessment of the patient's history is important.

Hematosalpinx appears on MRI as a hyperintense distention of the fallopian tube on fat-saturated T1- and T2-weighted images (Fig. 4.7). Low T2 signal intensity (T2-shading sign), often seen in endometriomas, is not characteristic of tubal endometriosis, maybe because tubal dilation is most commonly secondary to serosal/subserosal endometrial implants [32, 36, 37].

4.4 Deep Pelvic Endometriosis

Deep pelvic endometriosis (DPE) is defined as a subperitoneal invasion that exceeds 5 mm in depth in the retroperitoneal space or in the pelvic organ wall. DPE affects more frequently the rectovaginal septum and the uterosacral ligaments (69.2 %), vagina (14.5 %), alimentary tract (9.9 %), urinary tract (6.4 %), and other extraperitoneal pelvic sites [38].

From a clinical point of view, although peritoneal endometriosis can be asymptomatic, DPE is symptomatic in up to 75 % of cases. The symptoms are not specific, so an early diagnosis is a major challenge, as it can help to avoid mutilating surgery, enhance fertility, and improve quality of life [39–41].

From a pathological point of view, the endometrial glands and stroma infiltrate the adjacent fibromuscular tissue and elicit smooth muscle proliferation and fibrous reaction, with the development of solid tissue and nodules. In visceral organs the implants adhere to the serosal surface and can invade the muscular layers, eliciting smooth muscle proliferation, with consequent strictures and obstructions.

4.4.1 Diagnosis

Laparoscopy represents the gold standard in diagnosing and treating endometriosis because it provides a direct visualization of lesions that conduct to the most conservative surgical approach. However the laparoscopy cannot reach the subperitoneal plane, especially in presence of deep pelvic lesions with extensive adhesions and cul-de-sac obliteration. Because the standard treatment for DPE is complete surgical excision, presurgical diagnosis and accurate knowledge of location of the lesions are essential prerequisites for successful outcome. So in the preoperative assessment, a complete depiction of all pelvic planes with panoramic imaging techniques is extremely important. Several techniques have been used, including transabdominal, transvaginal, and transrectal ultrasonography (US), rectal endoscopic sonography, DBCE computed tomography (CT), and magnetic resonance (MR) imaging.

4.4.1.1 Ultrasonography

Transabdominal and transvaginal ultrasonography (US) is usually the first imaging technique used to diagnose endometriosis. The diagnosis of endometriomas and bladder endometriosis is reliable; recent studies have emphasized their role also in identifying deep endometriosis, especially when located in the rectal wall and retrocervical space [42]. However, their accuracy may vary depending on the lesions' location and the operator's experience.

Rectal endoscopic US with high-frequency probes has been recommended for diagnosing the depth of rectal wall infiltration [43–45], but it has poor penetration for the detection of other pelvic lesions, due to its small field of view. As in women with intestinal lesions, unifocal isolated localization accounts for only 21 % [46], and the ideal imaging method should be able to diagnose at least the associated pelvic lesions.

4.4.1.2 Double-Barium Contrast Enema (DBCE)

Double-barium contrast enema (DBCE) is rapidly available and low cost [47–50], and it has already been described as a valuable imaging tool in the preoperative diagnosis and quantification of bowel wall infiltration by endometriosic lesions. It demonstrates the extrinsic mass effect with the mucosal fine crenulation (Fig. 4.8f) and, if present, the stenosis of the lumen, findings highly suggestive of the presence of bowel endometriosis.

4.4.1.3 Multidetector Computed Tomography (MDCT)

MDCT has higher spatial resolution than MRI, but it involves radiation exposure and iodinated contrast medium administration to women of reproductive age, without the characterization of the hemoglobin degradation products, as MRI permits. MDCT identifies only aspecific signs, and it is generally employed in the acute complications of endometriosis, such as intestinal occlusion (Fig. 4.11f).

4.4.1.4 Magnetic Resonance Imaging (MRI)

MR imaging demonstrates high accuracy in the evaluation of DPE [19] and permits a complete survey of the anterior and posterior compartments of the pelvis. It is a noninvasive method with high spatial resolution and good tissue characterization.

The MRI diagnosis of DPE is established by the coexistence of *signal intensity abnormality* and *morphologic abnormalities* [19].

The *signal intensity* of DPE lesions is strictly related to the anatomo-pathological features. The acellular regions of fibrous tissue and smooth muscle proliferation have intermediate signal intensity on T1-weighted MR images and low signal intensity on T2-weighted images [51]. So the solid endometriosic lesions appear as hypointense masses on T2-weighted images with irregular indistinct or stellate margins, or as irregular hypointense soft tissue thickening, with or without nodular aspect. In particular, the involvement of such structures as uterosacral ligaments (USLs) and vaginal, rectal, or bladder walls may be suspected when they have a hypointense thickened, with or without nodular appearance on T2-weighted images [52].
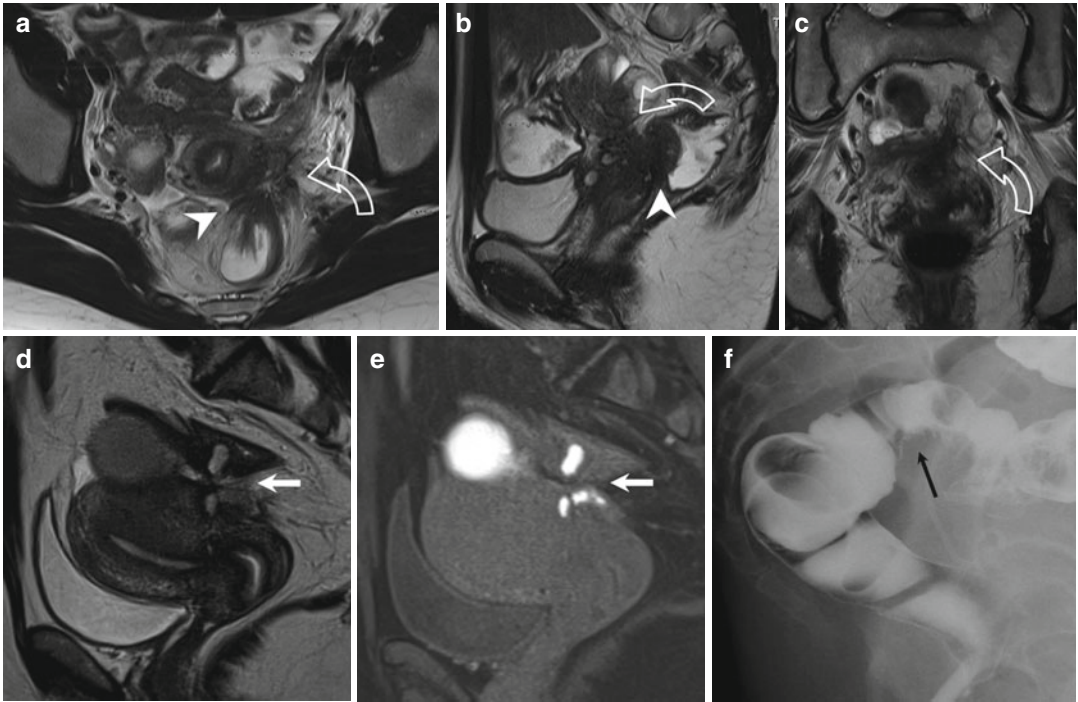
Fig. 4.8 Deep pelvic endometriosis (DPE). Two cases. (**a**–**c**) Axial (**a**), sagittal (**b**), and coronal (**c**) T2-weighted FSE images (TR 4670, TE 94) show a endometriosic lesion with stellate morphology (*curved arrow*), dishomogeneously hypointense, involving the left torus uterinus, the homolateral uterosacral ligament, the posterior wall of the uterine cervix and the anterior wall of the rectum (*arrowhead*). An obliteration of the Pouch of Douglas is present, with speculated low-signal-intensity strandings that obscure organ interfaces (adhesions). (**d**–**f**) Sagittal T2-weighted FSE images (**d**: TR 4670, TE 94), fat-saturated T1-weighted image (**e**: TR 369, TE 10) and double-barium contrast enema (DBCE: **f**). The lesion (*arrows*) presents some hemorrhagic components, hyperintense on T1-weighted images. It involves the posterior uterine wall and the above bowel with obliteration of the fat tissue plan between them. The involvement of the sigmoid colon is confirmed by the DBCE (**e**): it presents a focal irregular mucosal fine crenulation (*black arrow*) and a mild luminal stenosis

The presence of punctate foci of high signal intensity on T1-weighted images, more evident in the fat-suppressed sequences (Figs. 4.7d, e and 4.8e), represents regions of hemorrhage, because the ectopic endometrium responds to hormonal stimulation like basal endometrium. These hemorrhagic foci, hyperintense on T1-weighted images, may be distinguished from flow-related phenomena in the pelvic venous system.

Moreover intermingled hyperintense foci on T2-weighted images may be visible, for the presence of dilated ectopic endometrial glands (Figs. 4.7a and 4.9a).

Some masses of endometriosis are composed of a large proportion of glandular material with little fibrotic reaction, resulting in high-signal-intensity masses on T2-weighted images.

DPE can affect the anterior or the posterior compartment. The less frequently encountered anterior DPE is characterized by endometrial implants located anterior to the uterus [31], instead of the more frequent posterior DPE, characterized by lesions located posterior to the uterus.

The *morphologic abnormalities* vary according to the anatomic locations of endometriosis in the posterior and anterior compartment.

4.5 Endometriosis of the Anterior Compartment

It includes endometrial implants within the vesicouterine pouch, vesicovaginal septum, bladder (detrusor muscle), ureters, urethra, and, more
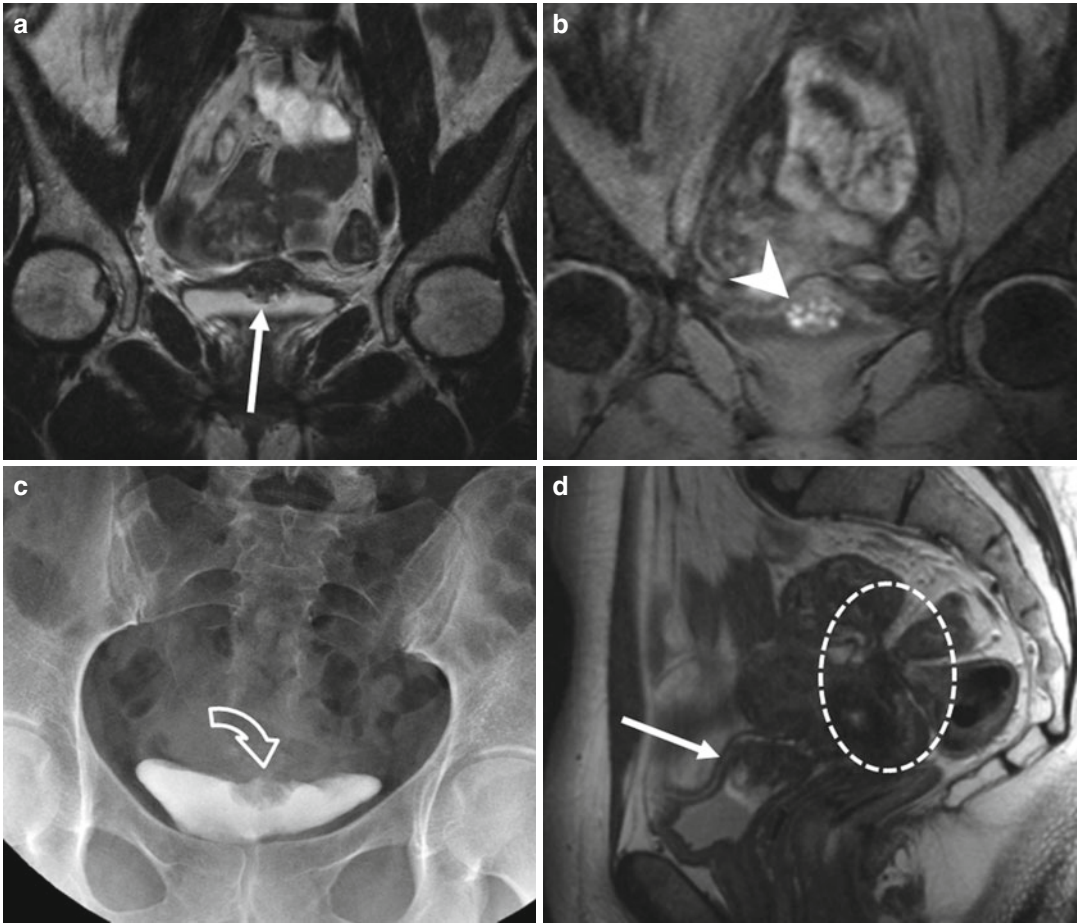
Fig. 4.9 Intrinsic bladder endometriosis (**a–d**). Coronal (**a**) and sagittal- (**d**) T2-weighted FSE MR images (TR 5390, TE 113); coronal fat-suppressed T1-weighted FSE image (**b**: TR 493, TE 4.9). A well-defined nodule is recognizable in the supero-posterior bladder wall (*arrows*); it infiltrates the bladder's dome and projects into the lumen (*intrinsic endometriosis*). On T1-weighted image (**b**), small-intermingled hyperintense foci are present within the nodule (*arrowhead*), finding consistent with bloody content within the ectopic endometrial glands. This aspect is crucial for the differential diagnosis between bladder endometriosis and bladder cancer. The excretory urographic study (**c**) shows the corresponding filling defect on the bladder's dome (*curved arrow*); this radiographic appearance is nonspecific for intrinsic bladder endometriosis and requires endoscopy and biopsy to rule out malignancy. Endometriosis of the posterior compartment coexists (**d**: *dashed circle*), with partial obliteration of the pouch of Douglas, infiltration of the posterior uterine surface and of the anterior rectosigmoid wall (*deep pelvic endometriosis*)

rarely, in the anterior pelvic wall (discussed in the *unusual locations*).

Endometriosis of the urinary tract is associated with lesions in other pelvic locations in up to 50–75 % of cases; it represents 0.2–2.5 % of all cases of endometriosis, with a frequency ratio of 40:5:1 for the bladder, ureters, and kidneys, respectively.

It has been showed that patients with ureteral and bladder endometriosis have more advanced stages of the disease (stages III and IV according to the 1996 American Society of Reproductive Medicine criteria) than patients without urinary system involvement.

• *Vesicouterine pouch* lesions are characterized by hypointense tissue on T2-weighted images, with or without nodular appearance, located on the anterior uterine surface, forming an obtuse angle with the vesical wall (Figs. 4.7a–c and 4.9d). The resulting extensive adhesions

between the peritoneum of the bladder fold and the uterus determine anteflexion of the uterus and obliteration of the vesicouterine pouch with the disappearance of the intervesicouterine fat [53].

The diagnosis is easier when the lesion is nodular, whereas it could be more difficult in case of plaque-like lesion [54].

- *Bladder* endometriosis can be seen at MRI as localized or diffuse hypointense thickening of the vesical wall on T2-weighted images with irregular margins that replaces the normal signal of detrusor muscle (Figs. 4.7 and 4.9). Eventually, intermingled hyperintense foci may be observed on T2-weighted (Fig. 4.7a, c) and T1-weighted fat-suppressed (Fig. 4.7d, e) images, findings that correspond to the dilated endometrial glands and blood content, respectively.

  The endometriosic implants of the bladder are more frequently confined to the serosal surface ("extrinsic" involvement: Fig. 4.7), but they can infiltrate the muscular layer appearing as mural masses projecting into the lumen ("intrinsic" involvement: Fig. 4.9) [3].

  Differential diagnosis: bladder endometriosis, appearing as localized wall thickening with occasional protrusion inside the bladder lumen, mimics bladder cancer [55]. Subserosal anterior leiomyoma of the uterus with extrinsic compression of the bladder is another differential diagnosis. The presence of intralesional hyperintense foci on T1-weighted images helps in the differential diagnosis.

- The *ureteral* involvement is usually unilateral, in its pelvic portion, and it is more frequently extrinsic (75–80 %) with endometrial tissue originating from adjacent structures that compress the ureter from the outside or that invade the adventitia and the surrounding connective tissue. The intrinsic involvement of the ureters is more rare (20–25 %) and is characterized by the presence of endometrial tissue in the muscular and/or mucosal layer of the ureter [56]. Ureteral endometriosis appears as irregular hypointense nodules on T2-weighted images with obliteration of the fat tissue plan between

nodule and ureter (Fig. 4.10d). Retractile adhesions may be visible as periureteral hypointense lines with angular deviation. Ureteral involvement may result in luminal narrowing with upstream dilatation of the ureter (Figs. 4.7a, b and 4.10a, b), hydronephrosis, and impairment of renal function, observed in up to 30 % of cases [57]. Findings at intravenous pyelography or MR urography are nonspecific and usually correspond to hydronephrosis with a stricture of the distal ureter. It is important to identify the ureter's involvement because it requires ureteral diversion or reimplantation surgery, with the presence of the urologist needed during surgical treatment.

- The *vesicovaginal septum* can be affected with a cystic lesion that resembles an endometrioma.

- *Urethral* endometriosis usually develops as contiguous extension from bladder lesions, while isolated forms are not reported in literature [53].

4.6 Endometriosis of the Posterior Compartment

It can involve the pouch of Douglas, the torus uterinus, the uterosacral ligaments (USLs), the vagina, the posterior vaginal fornix, the rectovaginal septum, and the bowel wall.

- Deep solid lesions involving the *pouch of Douglas* usually appear as ill-defined, hypointense tissue thickening on T2-weighted images, with possible hyperintense foci on T1-weighted sequences, reflecting the blood content (Fig. 4.8e). A partial or complete cul-de-sac obliteration can occur [58].

- The *torus uterinus* is a small transverse thickening that binds the insertion of both USLs on the posterior wall of the uterus. It is not clearly visible at MRI in absence of pathological thickening; it is frequently involved in endometriosis appearing as a mass or a thickening in the upper middle portion of the posterior cervix (Figs. 4.8a and 4.10d), forming an arciform abnormality. Uterine retroversion or
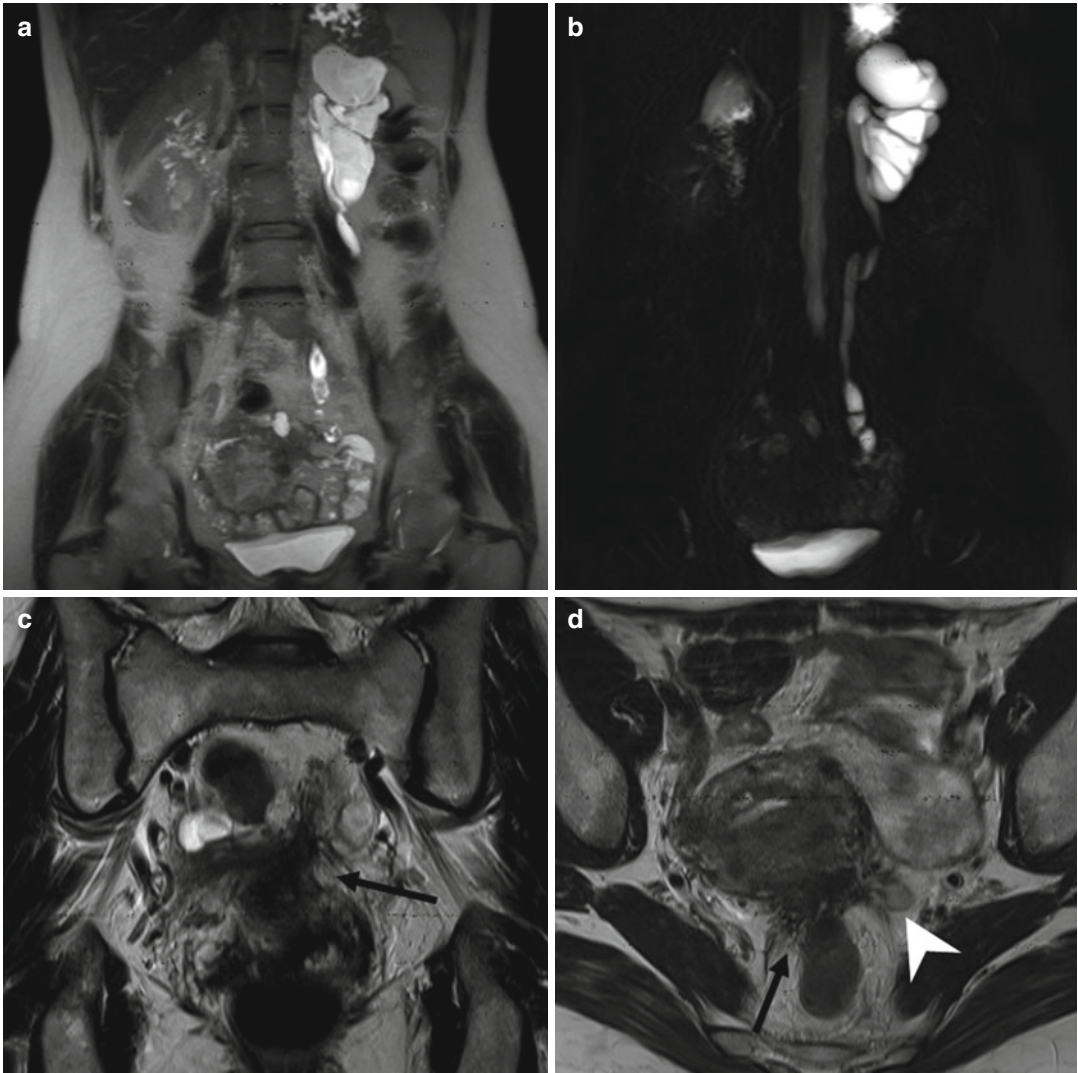
Fig. 4.10 Deep pelvic endometriosis involving the left ureter. Coronal (**a**, **c**: TR 4670, TE 94) and axial (**d**: TR 4070, TE 94) T2-weighted images; magnetic resonance urography (**b**: T2-haste thick slab, TR 6000, TE 754). There is a dilation of the left ureter and calyceal system (**a**, **b**) caused by a deep infiltrating lesion located in the posterior pelvic compartment (**c**, **d**: *black arrows*). The distal portion of the left ureter (**d**: *arrowhead*) is encased by the endometriosic lesion, with an upstream dilation of the urinary system. The lesion is poorly marginated, presents a stellate morphology, and involves also the posterior uterine surface and the anterior bowel wall

angular rectal attraction is often associated, reflecting the fibrotic component [59].

- The *uterosacral ligaments (USLs)* are normally visible at MR imaging as thin semicircular hypointense cords that originate from the lateral margin of the uterine cervix, directed dorso-cranially toward the sacrum. Normally, if visible, they appear thin and regular. When the USLs are involved by endometriosis, more frequently in their proximal part, their fibrotic thickening or the presence of a nodule within the ligaments, with regular or stellate margins (Figs. 4.8a and 4.10d), makes the ligaments palpable at physical examination. False-negative or false-positive results are possible when a retroflexed uterus, adhesions, or endometriomas mask the origin or the proximal part of the USL or in case of frozen pelvis [60].

Furthermore, thickened USLs due to endometriosis may be distinguished from the consequences of preview surgery.

- *Rectovaginal septum (RVS)* lesions account for 10 % of cases, and they consist of a nodule or a mass that passes through the lower border of the posterior lip of the cervix with attraction of the vaginal fornix. RVS lesions are usually associated with cul-de-sac obliteration and are, in most cases, secondary to involvement of the peritoneum of the pouch of Douglas. This is related to the embryogenetic origin of the RVS that originates from the fusion of the two layers of the peritoneal cul-de-sac extending downward between the rectum and the vaginal wall to the level of levator ani muscle.

- The involvement of the *cervix* appears as a thickening or a mass, hypointense on T2-weighted images, obliterating the posterior vaginal or cervical wall (Figs. 4.7f and 4.8a, b). Errors can occur, especially in case of retroflexed uterus or frozen pelvis. The retrocervical area is a virtual extraperitoneal space behind the cervix, situated above the rectovaginal septum. Here the *posterior vaginal fornix* is the larger recess located posterior to the cervix, and normally it appears as a curved regular cavity. Its involvement in endometriosis account for 65 % of cases and appears as an upward attraction of the vaginal fornix toward the lesion [38].

- The *parametrium* consists of connective tissue forming a sheet containing the blood vessels, the ureter and the inferior hypogastric plexus, extending from the lateral surface of the cervix and vagina to the lateral pelvic wall in the frontal plane [61, 62]. Signs of parametral involvement are the presence of a low-signal-intensity area in the paracervical or paravaginal region on T2-weighted images and a pelvic wall or ureteral involvement [63].

- 5–27 % of women with pelvic endometriosis present *intestinal* localizations. The bowel endometriosis most commonly affects the rectosigmoid junction (70–85 %) [3, 64]. Less frequent sites are the appendix, cecum, and distal ileum [3, 65].

The implants are usually superficial, localized to the serosa on the antimesenteric edge of the bowel, but they can erode the subserosal layers, causing thickening and fibrosis of the muscularis propria. The implanted tissue only rarely invades the mucosa that is almost always intact; this is why the colonoscopy is often false negative. In response to cyclic hemorrhage, an inflammatory response can cause adhesions, bowel strictures, and gastrointestinal obstruction.

To identify the intestinal lesions in the MRI study, we considered both *direct* and *indirect* signs. The *direct* signs consist of parietal nodules or plaques with low signal intensity on T2-weighted images and high signal foci on T1-weighted images (Figs. 4.7f and 4.8). The *indirect* signs include adhesions between the lesion, uterus, and/or adjacent organs (Fig. 4.3) with strands of hypointense tissue on T2-weighted images in the pelvic adipose tissue, abnormal angulations of bowel loops, and retroverted fixation of the uterus with obliteration of the posterior cul-de-sac (Figs. 4.7, 4.8, 4.9d, and 4.10c, d) [58].

The presence of hypointense parietal thickening on T2-weighted images (Figs. 4.7f and 4.8b), with or without intermingled hemorrhagic foci hyperintense on T1-weighted images, causes the disappearance of the hypointense signal of the anterior bowel wall and obliteration of the fat tissue plan. In most cases, the rectum is attracted toward the torus uterinus with involvement of the USL and obliteration of the cul-de-sac.

MR imaging has a good sensitivies and specificities, of 76.5–88.3 % and 76–80 %, respectively, in the diagnosis of rectosigmoid colon involvement [19, 42, 66, 67].

There is not consensus concerning the indications of gadolinium administration in the diagnosis of DPE. Use of contrast-enhanced MRI is primarily required to identify solid enhancing nodules in the endometriosic cysts, when malignant transformation is suspected. Contrast medium is also useful to define the extent of glandular tissue, fibrosis, and active inflammatory reaction [38] incited by micro- or macroscopic endometrial implants. However gadolinium is usually not administered because

implants of DPE can enhance, but it is neither sensitive nor specific [68]. Furthermore, an accurate preoperative evaluation of endometriosis extension has been demonstrated even without use of contrast agent [69, 70].

Opacification of rectum with air [64], water enema [71], or US gel [70] improves diagnostic capabilities of pelvic MRI, because it reaches a better contrast between the lumen and the wall of the rectus and a better delineation of the rectovaginal septum [43, 70]. Anyway with the MRI study, it is difficult to determine the depth of bowel wall infiltration and to differentiate lesions limited to the serosa from lesions that invade the muscular wall.

Differential diagnosis: radiographic findings of intestinal endometriosis may mimic a colon carcinoma as endometriosis causes marked overgrowth of the external muscular layer, producing an eccentric or a circumferential lesion, with crenulated appearance at BDCE. Unlike colonic carcinoma, endometriosis does not cause mucosal ulceration, and the mucosa is intact. Furthermore, the US and CT appearance are nonspecific, and they do not help in the differential diagnosis. MRI is a good tool in the differentiation between tumors and endometriosis in selected cases, thanks to the peculiar MRI signal intensity of endometriosic implants [72]. The differential diagnosis of the gastrointestinal implants includes also metastatic disease, in particular drop metastasis from an upper abdominal malignancy.

4.7   Complications of Endometriosis

The endometriosic implants can lead to a number of complications.

Adhesions represent a very common and clinically important complication and can result in intestinal obstruction (Fig. 4.11f). They occasionally can be identified on MRI as speculated low-signal-intensity strandings that obscure organ interfaces (Figs. 4.7a, 4.8a, 4.9d, and 4.10c, d). Indirect signs of adhesions include angulation of bowel loops (Fig. 4.9d), too large changes in

bowel diameter with peritoneal nodules, fixed posterior displacement of uterus and ovaries, elevation of the posterior vaginal fornix, loculated fluid collections, and hydrosalpinx [3].

Frozen pelvis is due to the extension of endometriosis to multiple adjacent pelvic structures, with a block of tissue that simulates a carcinoma [19]. Rupture of an endometrioma can lead to *hemoperitoneum. Ascites* can be a consequence of the rupture of endometriosic implant and subsequent peritoneal irritation. *Adnexal torsion* can be due to an endometrioma acting as a leading mass [73]. *Malignant transformation* is rare (<1 % cases of endometriosis), and long-standing ovarian endometrioma is most likely to undergo this change rather than extraovarian endometriosis [33, 35]. In fact, 75 % of malignant transformation arises from ovary and only 25 % from extraovarian lesions (endometrioid tumors and sarcomas) (Fig. 4.12).

4.8   Rare Locations of Endometriosis

Although extrapelvic endometriosis has been reported to affect almost all organs except the heart and the spleen, the most frequent location is in the abdominal wall [74].

4.8.1   Parietal Endometriosis

The principal risk factor for parietal endometriosis is antecedent abdominopelvic surgery [75–77], due to the iatrogenic seeding of endometrial cells within the scar tissue.

Parietal endometriosis of the abdomen is a rare finding, described in the rectus abdominis, umbilicus, sites of hysterectomy or cesarean scars, and puncture sites of amniocentesis or trocar for laparoscopy [75, 78, 79]. Solid endometriosis developing in *cesarean section scars*, after cesarean section, appears with hemorrhagic signal intensity in the context of the myometrium along the surgical scar (Fig. 4.11a, b) [80]. Endometriosis occurring on *episiotomy scars* has very a similar pathophysiology [81].
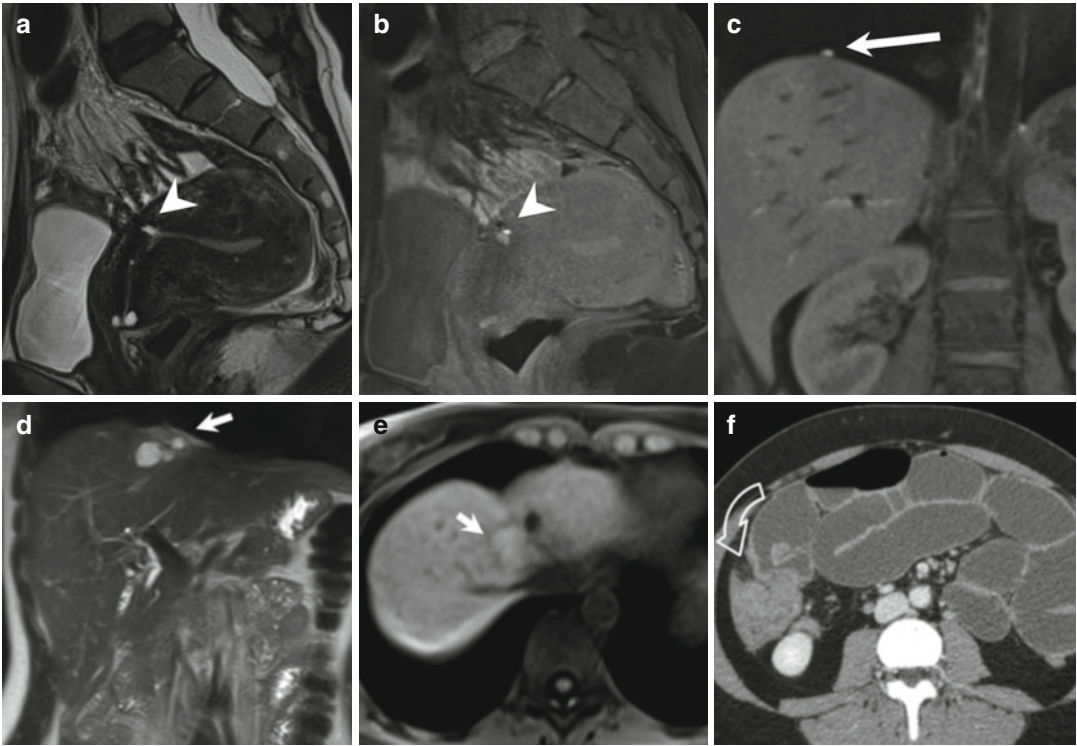
Fig. 4.11 Unusual locations. Endometriosis of the cesarean scar (**a**, **b**). Sagittal T2-weighted FSE images (**a**: TR 4670, TE 94) and T1-weighted FS-GRE image (**b**: TR 369, TE 10). Woman with previous cesarean section presents an endometriosic lesion (*arrowheads*) in the context of the myometrium, along the surgical scar. This lesion presents hyperintense foci on the T1-FS-weighted image, due to its hemorrhagic content. Diaphragmatic location (**c**: TR 541, TE 6.3). A millimetric hyperintense nodule on T1-weighted FS-GRE image (*arrow*) is recognizable on the right emidiaphragm, over the liver. (**d**, **e**) Diaphragmatic/hepatic locations. In this patient the right emidiaphragm is focally irregular and thickened (*arrow*)

due to previous surgery for endometriosic location. In this site a multiloculated lesion, hyperintense on the T2- (**d**: TR 1300, TE 88) and T1-weighted (**e**: TR 761, TE 5.9) images is recognizable. The anatomo-pathological examination after surgery demonstrated was an endometriosic lesion. MDCT technique axial image after intravenous contrast medium administration during portal phase (**f**) of a patient with endometriosis and bowel occlusion. The small bowel is dilated by fluid, and solid tissue is recognizable on the right flank (*curved arrow*). The patient underwent surgery, and the solid tissue was demonstrated as endometriosic lesion adherent to bowel walls, causing occlusion

4.8.2 Inguinal Endometriosis

It is more frequently located through the canal of Nuck, which, if patent, creates a communication between the peritoneal cavity and the inguinal canal [82]. The canal of Nuck is an embryological remnant of the peritoneovaginal canal; in women the round ligament extends toward the subcutaneous tissue in this canal up to the labia majora. Endometriosis locations in the canal of Nuck are extremely rare and appear on MRI as fibrohemorrhagic lesions in proximity to the inguinal ring (Fig. 4.13c, d). In these cases, the clinical presentation is pathognomonic

with a palpable inguinal mass intermittently painful following the menstrual cycle [83, 84]. The intra- and extraperitoneal portion of the round ligament, hernia sacs, and postoperative scars of the abdominal wall has been cited as regions of endometrial involvement in the groin.

4.8.3 Round Ligament Endometriosis

The round ligaments of the uterus originate at the uterine horns, where the uterus and the uterine
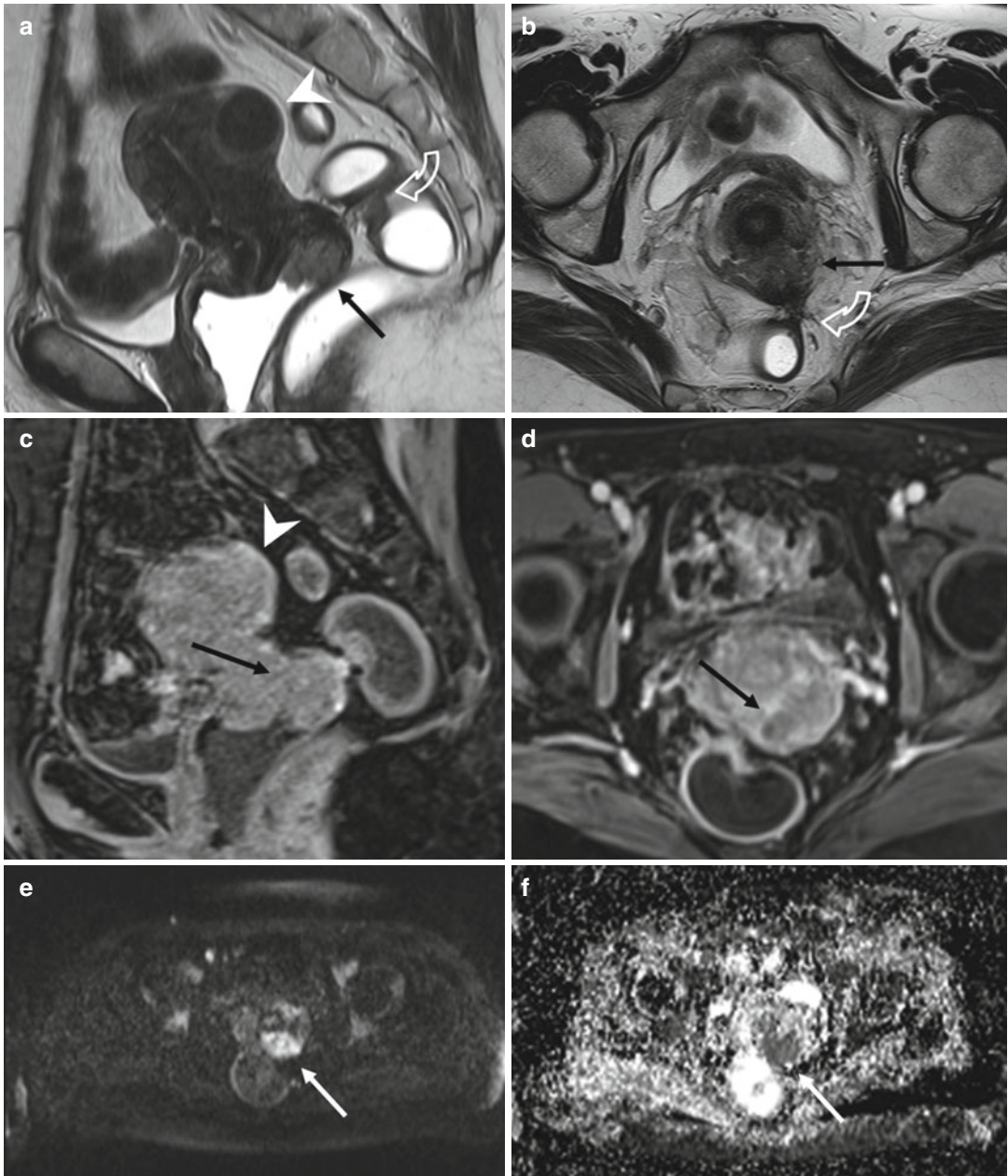
Fig. 4.12 Malignant transformation in endometriosis. Sagittal (**a**: TR 3857, TE 100) and axial (**b**: TR 3652, TE 100) T2-weighted MR images show a cervical lesion in the posterior fornix (*arrows*) in a patient with endometriosis of the posterior compartment (*curved arrows*). It exhibits enhancement on the T1-weighted image after contrast medium administration (**c**, **d**: TR 5.8, TE 2.8), and it shows restricted diffusion on diffusion-weighted ($b = 1,000$ s/mm^2) images (**e**) and apparent diffusion coefficient (ADC) maps (**f**). Also a subserosal leiomyoma of the posterior uterine wall is recognizable (*arrowheads*)

tube meet. These ligaments pass through the inguinal canals and enter the labium majus. The function of the round ligament is to maintain the anteversion of the uterus. Endometriosis of the round ligaments, either in their intra- or extra-peritoneal portions, is a rare event (0.3–0.6 %) [85]. It is located on the right side in more than 90 % of cases, probably due to the barrier to the menstrual flow reflux provided by the sigmoid colon on the left side [86]. On MRI, the round ligaments are thin structures with a fibrous signal intensity, anterior to the external iliac vessels.
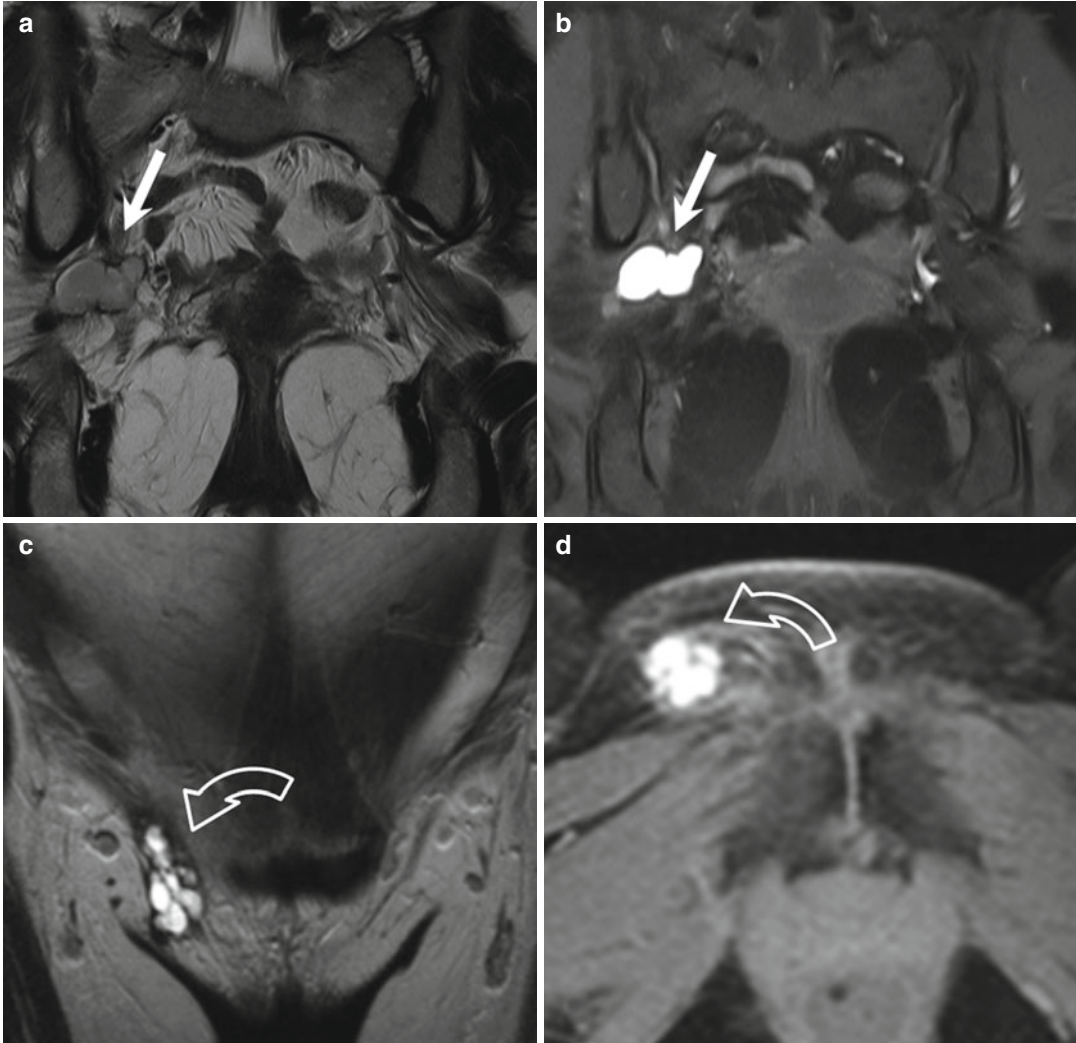

Fig. 4.13 Unusual locations. (**a**, **b**) Endometriosis of the ischiatic foramen. Coronal T2- (**a**: TR 5390, TE 113) and FS-T1-weighted (**b**: TR 369, TE 10) images. Woman with catamenial sciatica presents an endometriosic lesion in the ischiatic foramen (*arrows*), markedly hyperintense on T1-weighted sequence (**b**). (**c**, **d**) Endometriosis of the nuck canal. Coronal T2- (**c**: TR 5390, TE 113) and axial FS-T1-weighted (**d**: TR 822, TE 4.9) images. Woman with a painful palpable right inguinal mass presents a lesion near the right inguinal ring (*curved arrow*), multiloculated, with hemorrhagic content, hyperintense on T1- and T2-weighed images. It is an endometriosic location in the Nuck canal, where the round ligament extends toward the subcutaneous tissue. The round ligament is not involved. (**e**, **f**) Endometriosis of the right round ligament. Axial T2- (**e**: TR 5130, TE 108) and T1-weighted (**f**: TR 550, TE 9.3) images. The right round ligament appears thickened (*arrowhead*), irregular, hypointense in all pulsed sequences due to its fibrous thickening
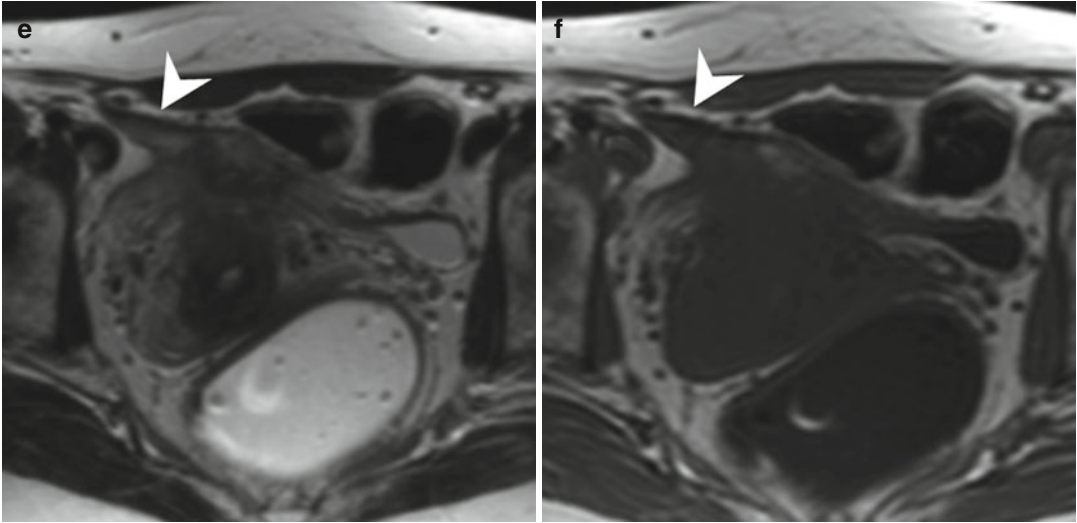
Fig. 4.13 (continued)

When involved by endometriosis, they appear as thickened, irregular, and with or without nodular appearance (Fig. 4.13e, f).

4.8.4 Sciatic Nerve Endometriosis (Cyclical Sciatica)

Cyclic sciatica due to implantation of endometrial tissue in the sciatic nerve in the region of the sciatic notch is a very unusual form of sciatica. It manifests as cyclic episodes of pain in the distribution of the sciatic nerve that coincide with menstruation. If not treated, a sensorimotor mononeuropathy of the sciatic nerve can develop [87]. MR imaging may show a focal mass-like lesion centered around the sciatic nerve, commonly in the area of the greater sciatic notch. This mass-like lesion often exhibits high signal intensity on T1-weighted images (more evident in the fat-suppressed T1-weighted images) and mixed signal intensity on T2-weighted images, depending upon the quantity, age, and proportion of hemorrhagic tissue (Fig. 4.13a, b).

4.8.5 Hepatic Endometriosis

Liver involvement by endometriosis is rare. Only 18 cases are reported in the English literature.

The pathogenesis is unknown; the blood/lymphatic dissemination, similar to the cancer metastasis, is the presumed pathway for intraparenchymal hepatic lesions [88, 89]. The imaging features of hepatic endometriosis are variable and depend on its response to the hormonal changes during menstrual cycles [90]. There is no magnetic resonance imaging (MRI)-specific characteristics, but most commonly it presents as well-defined lobulated cystic lesions (Fig. 4.11d, e) with possible solid components and septations [91, 92].

4.8.6 Thoracic Endometriosis (*Diaphragm, Pleura, Pericardium, and Lung*)

Endometriosis of the thorax is a clinical entity that includes the presence of ectopic endometrial tissue in the *diaphragm*, in the *pleura*, and rarely in the *pericardium. Diaphragmatic endometriosis* is a rare entity, often asymptomatic, in up to 90 % of cases associated with severe pelvic endometriosis. The most plausible theory about this condition is based on retrograde menstruation and subsequent transportation of viable cells in peritoneal fluid from the pelvis up the right paracolic gutter to the right hemidiaphragm. Here the cells are blocked by the falciform ligament and

infiltrate the right half of the muscle and then the left side, thus demonstrating its asymmetric distribution on the diaphragm. The lesions may be hide behind the right hepatic lobe (*perihepatic endometriosis:* Fig. 4.11c–e). Catamenial pneumothorax is the most common clinical expression [93].

4.8.7 Nasal Mucosa Endometriosis

It is an exceptional localization (two cases reported in the literature). The clinical symptoms are catamenial nasal tumefaction, pain, and epistaxis, and the endoscopic biopsy allows the diagnosis [94, 95].

References

1. Revised American Fertility Society classification of endometriosis: 1985 (1985) Fertil Steril 43(3):351–352
2. Brosens I et al (2004) Diagnosis of endometriosis: pelvic endoscopy and imaging techniques. Best Pract Res Clin Obstet Gynaecol 18(2):285–303
3. Woodward PJ, Sohaey R, Mezzetti TP Jr (2001) Endometriosis: radiologic-pathologic correlation. Radiographics 21(1):193–216; questionnaire 288–294
4. Spaczynski RZ, Duleba AJ (2003) Diagnosis of endometriosis. Semin Reprod Med 21(2):193–208
5. Vigano P et al (2004) Endometriosis: epidemiology and aetiological factors. Best Pract Res Clin Obstet Gynaecol 18(2):177–200
6. Olive DL, Henderson DY (1987) Endometriosis and mullerian anomalies. Obstet Gynecol 69(3 Pt 1):412–415
7. Clement PB (1990) Pathology of endometriosis. Pathol Annu 25(Pt 1):245–295
8. Halme J et al (1984) Retrograde menstruation in healthy women and in patients with endometriosis. Obstet Gynecol 64(2):151–154
9. Liu DT, Hitchcock A (1986) Endometriosis: its association with retrograde menstruation, dysmenorrhoea and tubal pathology. Br J Obstet Gynaecol 93(8):859–862
10. Jenkins S, Olive DL, Haney AF (1986) Endometriosis: pathogenetic implications of the anatomic distribution. Obstet Gynecol 67(3):335–338
11. Dunselman GA, Groothuis PG (2004) Etiology of endometriosis: hypotheses and facts. Gynecol Obstet Invest 57(1):42–43
12. Kurman RJ (2011) Diseases of the peritoneum. In: Blaustein's pathology of the female genital tract, 6th edn. Springer, New York/London
13. Kashima K et al (2004) Familial risk among Japanese patients with endometriosis. Int J Gynaecol Obstet 84(1):61–64
14. Rogers PA et al (2013) Defining future directions for endometriosis research: workshop report from the 2011 World Congress of Endometriosis in Montpellier, France. Reprod Sci 20(5):483–499
15. Carvalho LF et al (2013) From conception to birth – how endometriosis affects the development of each stage of reproductive life. Minerva Ginecol 65(2):181–198
16. Chapron C et al (2012) Ovarian endometrioma: severe pelvic pain is associated with deeply infiltrating endometriosis. Hum Reprod 27(3):702–711
17. Gauche Cazalis C et al (2012) Preoperative imaging of deeply infiltrating endometriosis in: transvaginal sonography, rectal endoscopic sonography and magnetic resonance imaging. Gynecol Obstet Fertil 40(11):634–641
18. Saba L et al (2012) MRI and "tenderness guided" transvaginal ultrasonography in the diagnosis of recto-sigmoid endometriosis. J Magn Reson Imaging 35(2):352–360
19. Bazot M et al (2004) Deep pelvic endometriosis: MR imaging for diagnosis and prediction of extension of disease. Radiology 232(2):379–389
20. Siegler AM, Camilien L (1994) Adenomyosis. J Reprod Med 39(11):841–853
21. Levy G et al (2013) An update on adenomyosis. Diagn Interv Imaging 94(1):3–25
22. Kishi Y et al (2012) Four subtypes of adenomyosis assessed by magnetic resonance imaging and their specification. Am J Obstet Gynecol 207(2):114 e1-7
23. Bazot M et al (2001) Ultrasonography compared with magnetic resonance imaging for the diagnosis of adenomyosis: correlation with histopathology. Hum Reprod 16(11):2427–2433
24. Reinhold C et al (1996) Diffuse adenomyosis: comparison of endovaginal US and MR imaging with histopathologic correlation. Radiology 199(1):151–158
25. Novellas S et al (2011) MRI characteristics of the uterine junctional zone: from normal to the diagnosis of adenomyosis. AJR Am J Roentgenol 196(5):1206–1213
26. Takeuchi M, Matsuzaki K, Nishitani H (2010) Manifestations of the female reproductive organs on MR images: changes induced by various physiologic states. Radiographics 30(4):1147
27. Utsunomiya D et al (2004) Endometrial carcinoma in adenomyosis: assessment of myometrial invasion on T2-weighted spin-echo and gadolinium-enhanced T1-weighted images. AJR Am J Roentgenol 182(2):399–404
28. Patel MD et al (1999) Endometriomas: diagnostic performance of US. Radiology 210(3):739–745
29. Togashi K et al (1991) Endometrial cysts: diagnosis with MR imaging. Radiology 180(1):73–78
30. Wu TT et al (2004) Magnetic resonance imaging of ovarian cancer arising in endometriomas. J Comput Assist Tomogr 28(6):836–838
31. Coutinho AC Jr et al (2011) Pelvic applications of diffusion magnetic resonance images. Magn Reson Imaging Clin N Am 19(1):133–157
32. Siegelman ES, Oliver ER (2012) MR imaging of endometriosis: ten imaging pearls. Radiographics 32(6):1675–1691

33. McDermott S et al (2012) MR imaging of malignancies arising in endometriomas and extraovarian endometriosis. Radiographics 32(3):845–863
34. Takeuchi M, Matsuzaki K, Nishitani H (2008) Magnetic resonance manifestations of decidualized endometriomas during pregnancy. J Comput Assist Tomogr 32(3):353–355
35. Takeuchi M et al (2006) Malignant transformation of pelvic endometriosis: MR imaging findings and pathologic correlation. Radiographics 26(2):407–417
36. Kim MY et al (2009) MR Imaging findings of hydrosalpinx: a comprehensive review. Radiographics 29(2):495–507
37. Rezvani M, Shaaban AM (2011) Fallopian tube disease in the nonpregnant patient. Radiographics 31(2):527–548
38. Del Frate C et al (2006) Deep retroperitoneal pelvic endometriosis: MR imaging appearance with laparoscopic correlation. Radiographics 26(6):1705–1718
39. Redwine DB, Wright JT (2001) Laparoscopic treatment of complete obliteration of the cul-de-sac associated with endometriosis: long-term follow-up of en bloc resection. Fertil Steril 76(2):358–365
40. Darai E et al (2005) Feasibility and clinical outcome of laparoscopic colorectal resection for endometriosis. Am J Obstet Gynecol 192(2):394–400
41. Darai E et al (2005) Fertility after laparoscopic colorectal resection for endometriosis: preliminary results. Fertil Steril 84(4):945–950
42. Abrao MS et al (2007) Comparison between clinical examination, transvaginal sonography and magnetic resonance imaging for the diagnosis of deep endometriosis. Hum Reprod 22(12):3092–3097
43. Kinkel K et al (1999) Magnetic resonance imaging characteristics of deep endometriosis. Hum Reprod 14(4):1080–1086
44. Chapron C et al (1998) Results and role of rectal endoscopic ultrasonography for patients with deep pelvic endometriosis. Hum Reprod 13(8):2266–2270
45. Fedele L et al (1998) Transrectal ultrasonography in the assessment of rectovaginal endometriosis. Obstet Gynecol 91(3):444–448
46. Chapron C et al (2003) Anatomical distribution of deeply infiltrating endometriosis: surgical implications and proposition for a classification. Hum Reprod 18(1):157–161
47. Faccioli N et al (2008) Barium enema evaluation of colonic involvement in endometriosis. AJR Am J Roentgenol 190(4):1050–1054
48. Rock JA (1995) The revised American Fertility Society classification of endometriosis: reproducibility of scoring. ZOLADEX Endometriosis Study Group. Fertil Steril 63(5):1108–1110
49. Prystowsky JB et al (1988) Gastrointestinal endometriosis. Incidence and indications for resection. Arch Surg 123(7):855–858
50. Landi S et al (2004) Preoperative double-contrast barium enema in patients with suspected intestinal endometriosis. J Am Assoc Gynecol Laparosc 11(2):223–228
51. Siegelman ES, Outwater EK (1999) Tissue characterization in the female pelvis by means of MR imaging. Radiology 212(1):5–18
52. Loubeyre P et al (2009) Anatomic distribution of posterior deeply infiltrating endometriosis on MRI after vaginal and rectal gel opacification. AJR Am J Roentgenol 192(6):1625–1631
53. Coutinho A Jr et al (2011) MR imaging in deep pelvic endometriosis: a pictorial essay. Radiographics 31(2):549–567
54. Savelli L et al (2009) Diagnostic accuracy and potential limitations of transvaginal sonography for bladder endometriosis. Ultrasound Obstet Gynecol 34(5):595–600
55. Kinkel K et al (2006) Diagnosis of endometriosis with imaging: a review. Eur Radiol 16(2):285–298
56. Frachet O et al (2006) Ureteral obstruction from endometriosis: a case report and review of the literature. J Gynecol Obstet Biol Reprod (Paris) 35 (5 Pt 1):500–503
57. Perez-Utrilla Perez M et al (2009) Urinary tract endometriosis: clinical, diagnostic, and therapeutic aspects. Urology 73(1):47–51
58. Kataoka ML et al (2005) Posterior cul-de-sac obliteration associated with endometriosis: MR imaging evaluation. Radiology 234(3):815–823
59. Kinkel K. (2005) Management of endometriosis. Informa Healthcare, Philadelphia, pp 448–451
60. Bazot M et al (2011) Value of thin-section oblique axial T2-weighted magnetic resonance images to assess uterosacral ligament endometriosis. Hum Reprod 26(2):346–353
61. Ercoli A et al (2005) Terminologia Anatomica versus unofficial descriptions and nomenclature of the fasciae and ligaments of the female pelvis: a dissection-based comparative study. Am J Obstet Gynecol 193(4):1565–1573
62. Touboul C et al (2008) The lateral infraureteral parametrium: myth or reality? Am J Obstet Gynecol 199(3):242 e1-6
63. Bazot M et al (2012) The value of MRI in assessing parametrial involvement in endometriosis. Hum Reprod 27(8):2352–2358
64. Faccioli N et al (2010) Evaluation of colonic involvement in endometriosis: double-contrast barium enema vs. magnetic resonance imaging. Abdom Imaging 35(4):414–421
65. Olive DL, Schwartz LB (1993) Endometriosis. N Engl J Med 328(24):1759–1769
66. Bazot M et al (2007) Accuracy of magnetic resonance imaging and rectal endoscopic sonography for the prediction of location of deep pelvic endometriosis. Hum Reprod 22(5):1457–1463
67. Chapron C et al (2004) Accuracy of rectal endoscopic ultrasonography and magnetic resonance imaging in the diagnosis of rectal involvement for patients presenting with deeply infiltrating endometriosis. Ultrasound Obstet Gynecol 24(2):175–179

68. Ascher SM et al (1995) Endometriosis: appearance and detection with conventional and contrast-enhanced fat-suppressed spin-echo techniques. J Magn Reson Imaging 5(3):251–257

69. Zanardi R et al (2003) Staging of pelvic endometriosis based on MRI findings versus laparoscopic classification according to the American Fertility Society. Abdom Imaging 28(5):733–742

70. Bazot M et al (2011) Deep pelvic endometriosis: limited additional diagnostic value of postcontrast in comparison with conventional MR images. Eur J Radiol 80(3):e331–e339

71. Scardapane A et al (2013) Deep pelvic endometriosis: accuracy of pelvic MRI completed by MR colonography. Radiol Med 118(2):323–338

72. Bis KG et al (1997) Pelvic endometriosis: MR imaging spectrum with laparoscopic correlation and diagnostic pitfalls. Radiographics 17(3):639–655

73. Sonavane SK, Kantawala KP, Menias CO (2011) Beyond the boundaries-endometriosis: typical and atypical locations. Curr Probl Diagn Radiol 40(6): 219–232

74. Tokue H, Tsushima Y, Endo K (2009) Magnetic resonance imaging findings of extrapelvic endometriosis of the round ligament. Jpn J Radiol 27(1):45–47

75. Novellas S et al (2010) Anterior pelvic endometriosis: MRI features. Abdom Imaging 35(6):742–749

76. Ideyi SC et al (2003) Spontaneous endometriosis of the abdominal wall. Dig Surg 20(3):246–248

77. Crespo R, Puig F, Marquina I (2005) Pyramidalis muscle endometriosis in absence of previous surgery. Int J Gynaecol Obstet 89(2):148–149

78. Hassanin-Negila A et al (2006) Endometriomas of the abdominal wall: imaging findings. J Radiol 87(11 Pt 1): 1691–1695

79. Zhao X et al (2005) Abdominal wall endometriomas. Int J Gynaecol Obstet 90(3):218–222

80. Gougoutas CA et al (2000) Pelvic endometriosis: various manifestations and MR imaging findings. AJR Am J Roentgenol 175(2):353–358

81. Gunes M et al (2005) Incisional endometriosis after cesarean section, episiotomy and other gynecologic procedures. J Obstet Gynaecol Res 31(5):471–475

82. Choudhary S et al (2009) Unusual imaging appearances of endometriosis. AJR Am J Roentgenol 192(6):1632–1644

83. Kirkpatrick A et al (2006) Radiologic-pathologic conference of Brooke Army Medical Center: endometriosis of the canal of Nuck. AJR Am J Roentgenol 186(1):56–57

84. Cervini P, Mahoney J, Wu L (2005) Endometriosis in the canal of Nuck: atypical manifestations in an unusual location. AJR Am J Roentgenol 185(1):284–285

85. Strasser EJ, Davis RM (1977) Extraperitoneal inguinal endometriosis. Am Surg 43(6):421–422

86. Mashfiqul MA, Tan YM, Chintana CW (2007) Endometriosis of the inguinal canal mimicking a hernia. Singapore Med J 48(6):e157–e159

87. Wadhwa V et al (2012) Sciatic nerve tumor and tumor-like lesions – uncommon pathologies. Skeletal Radiol 41(7):763–774

88. Goldsmith PJ et al (2009) Case hepatic endometriosis: a continuing diagnostic dilemma. HPB Surg 2009:407206

89. Keichel S et al (2011) Lymphangiogenesis in deep infiltrating endometriosis. Hum Reprod 26(10):2713–2720

90. Inal M et al (2000) Hepatic endometrioma: a case report and review of the literature. Eur Radiol 10(3): 431–434

91. Fluegen G et al (2013) Intrahepatic endometriosis as differential diagnosis: case report and literature review. World J Gastroenterol 19(29):4818–4822

92. Asran M, Rashid A, Szklaruk J (2010) Hepatic endometriosis mimicking metastatic disease: a case report and review of the literature. J Radiol Case Rep 4(11):26–31

93. Rousset-Jablonski C et al (2011) Catamenial pneumothorax and endometriosis-related pneumothorax: clinical features and risk factors. Hum Reprod 26(9): 2322–2329

94. Laghzaoui O, Laghzaoui M (2001) Nasal endometriosis: apropos of 1 case. J Gynecol Obstet Biol Reprod (Paris) 30(8):786–788

95. Mignemi G et al (2012) A case report of nasal endometriosis in a patient affected by Behcet's disease. J Minim Invasive Gynecol 19(4):514–516